Tampereen yliopisto

Arno Pammo

THE EFFECT OF A MECHANICAL STIMULUS ON ADHESION AND NUCLEI OF EPITHELIAL CELLS

Master's Thesis
Faculty of Medicine and Health Technology
Inspector: Sampo Tuukkanen
Inspector: Teemu Ihalainen
4/2020

ABSTRACT

Arno Pammo: The effect of a mechanical stimulus on adhesion and nuclei of epithelial cells
Master's Thesis
Tampere University
Biotechnology
4/2020

Cells' response to mechanical stimuli, mechanotransduction, is a biological phenomenon known to exist but not yet completely explained. In this thesis work the aim was to subject epithelial cells to mechanical stress and evaluate changes in their nuclear shape and adhesions between the cells. For this purpose, a novel cell vibration system was constructed. It was designed to fit into the microscope well plate holder. Movement was horizontal and generated with piezo actuators. The system included an accelerometer.

Canine kidney epithelial cells were vibrated at 70 Hz for 30 minutes, with peak acceleration of 1,35 *g*. Cells were then fixed and stained for chromatin and proteins associated with cell-cell adhesions and transcription regulation.

Microscope imaging showed increments in cell-cell adhesions. On the other hand, further analysis revealed that no meaningful changes in nuclear shape or yes-associated protein localization had occurred. Piezo elements' high resonant frequency forced the driver voltage to be low frequency and square wave. High frequencies would result in the test samples slipping inside the device. Still, the vibration system was considered a success. It could be modified to provide different ranges of motion and work as a useful tool in cell adhesion and mechanotransduction research.

Keywords: mechanotransduction, cell adhesion, epithelium, cell vibration.

TIIVISTELMÄ

Arno Pammo: Mekaanisen ärsytyksen vaikutus epiteelisolujen adheesioon ja tumaan
Diplomityö
Tampereen Yliopisto
Biotekniikka
04/2020

Solujen kyky reagoida mekaaniseen ärsytykseen on ilmiönä tunnettu, mutta toistaiseksi sen yksityiskohtia ei täydellisesti ole selitetty. Tämän työn tavoitteena oli tutkia, millaisia vasteita epiteelisoluissa havaitaan niiden adheesiossa ja tumassa, kun ne altistetaan tärinälle. Tarkoitusta varten rakennettiin järjestelmä, jolla soluja voitiin tärisyttää. Se mitoitettiin mahtumaan mikroskoopin kuoppalevyille tarkoitetulle näytetasolle. Vaakasuuntainen liike tuotettiin pietsoelementeillä. Solutäristin sisälsi myös kiihtyvyysanturin.

Koiran munuaisen epiteelisoluja altistettiin 70 Hz:n tärinälle 30 minuutin ajan, huippukiihtyvyyden ollessa 1,35 *g*. Tämän jälkeen solut fiksattiin ja niistä leimattiin adheesioproteiineja, kromatiini ja transkriptiosäätelijöitä.

Mikroskooppikuvien perusteella solujen väliset liitokset lisääntyivät. Tarkemman analyysin perusteella solujen tumien muoto ja YAP-regulaattorin sijainti eivät muuttuneet merkittävästi. Pietsoelementtien korkea resonanssitaajuus rajoitti käytettävän jännitteen matalataajuiseksi kanttiaalloksi. Suurilla taajuuksilla soluastian ja täristimen välinen kitka ei ollut riittävä. Tästä huolimatta solutäristäjää voitiin pitää onnistuneena. Pienin muutoksin tärinän amplitudia on mahdollista muuttaa, ja laite voisi hyvin toimia työkaluna solututkimuksessa.

Avainsanat: mekanotransduktio, soluadheesio, solujen täristäminen, epiteeli.

FOREWORD

This thesis work was done in Tampere University Faculty of Medicine and Health Technology to finalize my studies in bioimaging and -measurements.

I would like to express my gratitude and thank the following people: my supervisors Teemu Ihalainen and Sampo Tuukkanen for their guidance during this work, Elina Mäntylä for all the help in cell culturing and imaging, Juhani Virtanen for his advice on device construction and Vesa Virtanen for his work with accelerometer characterization and programming.

Tampere, 21.4.2020

Arno Pammo

TABLE OF CONTENTS

LIST OF ABBREVIATIONS

DAPI	4′,6-diamidino-2-phenylindole
ECM	Extracellular matrix
FAK	Focal adhesion kinase
GPTase	Guanosine triphosphate hydrolyzer
IgCAM	Immunoglobulin family cell adhesion molecule
LAP	Lamina associated protein
LINC	Linker of nucleoskeleton and cytoskeleton
MetOH	Methanol
MDCK	Madin-Darby canine kidney
PFA	Paraformaldehyde
PLA	Polylactic acid
PDMS	Polydimethylsiloxane
PZT	Lead zirconate titanate
SRF	Serum response factor
SUN	Sad1p, UNC-84 domain in a protein
TAZ	Transcriptional coactivator with PDZ-binding motif
YAP	Yes-associated protein

1. INTRODUCTION

Without being able to bind to each other or their surroundings, cells could not form functioning organs (Bray *et al.*, 2009; Pollard, 2017). Even single cells, for example white blood cells, attach to and detach from surfaces and move across them (Hynes, 1992; Pollard, 2017). In this case the adhesion is transient and easily reversible. Stronger binding is needed in supporting tissues and epithelium to endure external forces and to form tight seals (Bray *et al.*, 2009). While cells can control the adhesion and binding mechanisms to certain extent, adhesions and bindings affect the cell too. The receptors on the cell membrane are interconnected to the cytoskeleton and indirectly up to the nucleus. External mechanical stimuli have been shown to affect the nucleus' physical shape and gene expression, via a phenomenon called mechanotransduction (Dahl, Ribeiro and Lammerding, 2008; Wang, Tytell and Ingber, 2009; Rustad, Wong and Gurtner, 2013; Szczesny and Mauck, 2016; Vining and Mooney, 2017). Strengthening of bones and thickening of skin are well known examples of human body responding to physical stress. Physical exercise helps to maintain bone mass and prevents osteoporosis in older age (U.S. Department of Health and Human Services, no date; Drinkwater, 1994). Similarly, the skin thickens if it is affected by physical stress, e.g. on one's soles after walking long distances regularly (American Physical Therapy Association., 2001; Mueller and Maluf, 2002).

Studying cell adhesion and mechanotransduction is important not only to gain new knowledge of cell differentiation and the human biological system, but also for healthcare and therapy reasons. Cell adhesion is studied to find new information and innovation for applications in cellular biology and biomedical engineering fields (Khalili and Ahmad, 2015). These new findings also help to scientifically evaluate old therapy methods. For example, the so called "whole-body vibration exercise" that was marketed to strengthen bones and muscles and to stimulate the production of anabolic hormones, did not affect human body enough to be considered a valid weight loss method (Di Loreto *et al.*, 2004). In the light of new studies, vibrational therapies might still be possible. Vibrations from vocal folds are thought to influence the close by thyroid gland quite significantly which can affect the endocrine system (Wagner *et al.*, 2016). There exist a few medical disorders relating to cell adhesion, such as leukocyte adhesion deficiency or Bernard-Soulier syndrome (Pollard, 2017). The former appears as white blood cells being

incapable to bind to the inner lining of blood vessels or migrate to infected regions in the connective tissue. Bernard-Soulier syndrome is a bleeding disorder, where blood platelets do not aggregate properly. In addition, cell adhesion is relevant to formation of tumor metastasis (Hirohashi and Kanai, 2004; Kawaguchi, 2016). Being involved in cancer progression and metastasis is also true for mechanotransduction, however it is more relevant in developmental disorders in bone and muscle tissue (Jaalouk and Lammerding, 2009). Work-related diseases are also present in mechanotransduction category: a vibratory impact, such as that from continuously holding and operating power tools, can cause hand-arm vibration syndrome (HAVS) which involves damage to blood vessels, muscles and nerves in upper extremities (Rolke *et al.*, 2013).

Recent research in the field is rather broad, as there are some papers focusing on the smaller details and others concentrating on the implementation of mechanotransduction related methods as part of therapy or cell differentiation. Glatt et al. (2019) state that currently clinical applications utilizing mechanotransduction are limited in their number, albeit it is widely known that bone and cartilage would respond to mechanical stress well. They demonstrate that modulating the mechanical environment of damaged bone tissue soon after the injury will improve the healing process significantly. However, the details behind the phenomena are not fully understood and further studies are required (Glatt, Evans and Stoddart, 2019). Mechanotransduction's importance in the development of cancer has been recently studied by Ayad et al. and Bauer et al. Changes in tissue and cell mechanics, i.e. the way they sense and interpret mechanical signals, are linked to cancer and cardiovascular disease. Focal adhesion kinase (FAK) serve as key integrator of signals from growth factors and cell adhesion, and they are overly expressed in cancer frequently. Bauer et al. demonstrate how FAK can undergo conformational changes due to mechanical forces, causing them to activate and create adhesion signaling. Ayad et al. discuss new technology to enable measurements of mechanical properties of cells and tissue and difficulties within their implementation (Ayad, Kaushik and Weaver, 2019; Bauer *et al.*, 2019). Similarly to FAK, the inflammasomes' activation may be influenced by cell mechanical environment, according to Joshi and Morley (2019) (Joshi and Morley, 2019). In addition, Burridge et al. (2019) say the mechanical environment affects the cell adhesion molecules, which regulate signaling pathway of a GPTase (guanosine triphosphate hydrolyzer) enzyme. They also discuss how evidence implies that cell nucleus physically connected to the cytoskeleton contributes to the overall level of tension generated within the cytoskeleton (Burridge, Monaghan-Benson and Graham, 2019). Furthermore, roles of other cell organelles in mechanotransduction are being uncovered. Le Roux et al. (2019) state that plasma membrane is a major component in

transducing mechanical signals to chemical responses inside the cell (Le Roux *et al.*, 2019). Common to all recent publications is that the authors emphasize the disclarity of the details in e.g. transduced signal pathways and the need for additional research. Methods to subject the cells for external stress for research purposes are diverse. They include loudspeaker elements (Tirkkonen *et al.*, 2011), special bioreactors (Tsimbouri *et al.*, 2017), micropipettes (Grasland-Mongrain *et al.*, 2018) and even industrial vibration calibrator originally meant for sensor testing (Kanie *et al.*, 2019). In addition, a more simplistic method is to place a glass disc on top of the cells to compress them (Ullrich *et al.*, 2019). Cell stretching studies have enjoyed the option to use commercial purpose-built devices (Hornberger *et al.*, 2005; Huang *et al.*, 2013).

Goal for this thesis work was to create a system that could be used in mechanotransduction and adhesion studies by inducing cyclic movement to living cells while they are monitored under a microscope, and eventually test the shaker device in a real application and evaluate the effect of vibration in the epithelial cells. It was expected that the generated movement would result in visible changes in epithelial cells and weakly attached cells would come loose from the substrate. The cells were chosen to be canine kidney epithelial cells. Considering the properties epithelium represents and environmental aspects related to it, it is an interesting study subject for adhesion and mechanotransduction research. Epithelium presents the source of cancer in 90% of the cases (Frank, 2018). Epithelium has a high level of cell division and it is exposed to external harm more so than other tissues, which explain the higher cancer occurrence (Bray *et al.*, 2009; Frank, 2018). In addition to this, there exist many well defined epithelial cell lines that are used in research (Freshney and Freshney, 2002).

The structure of this thesis is as follows: in Chapter 2 the basics of cell adhesion, mechanotransduction and epithelium are presented. Piezoelectric effect is explained briefly. In Chapter 3 the vibration system design and construction are explained as well as the cell culture and test methodologies. Test results are presented in Chapter 4. In Chapter 5, the results discussed, and the testing methodology compared to other publications. Lastly in Chapter 6 the conclusion and future prospects are given.

2. THEORY

2.1 Cell adhesion

Cell adhesion is related to the ability of a single cell to adhere to neighboring cells or the surrounding environment, the extracellular matrix (ECM). Almost every cell type interacts with the molecules in their environment, often binding to them with the adhesion proteins on their cell membrane. Adhesion is essential for many signaling cascades and intercellular communication as well as forming of tissues. Many adhesion receptors are connected to the cytoskeleton and interact with it. Without this, there would not be structural strength in e.g. muscles. Interaction between surface receptors and cytoskeleton can activate intracellular signal transduction. When a ligand binds to a receptor, it can lead to changes in gene expression, cellular differentiation, secretion, motility, receptor activation and cell division (Pollard, 2017). In passive *in vitro* adhesion where the cell adheres to static surface, e.g. that of a culture dish, the cell flattens and spreads on the surface. The cytoskeleton is actively reorganized and it changes the cell's morphology (Lebaron and Athanasiou, 2000). Most cells are anchorage-dependent, meaning they are not viable if they are unattached to each other or a surface. Cell adhesion is defined by plasma membrane receptors that are selectively expressed by cells. Cells can recognize surfaces and selectively interact with each other using their adhesion receptors (Pollard, 2017). In developing cells, the connections with extracellular matrix and other cells specify and regulate their differentiation. During embryonic development, cells associate with cells of the same type. In fact, they are able to sort themselves in *in vitro* conditions, where the different cells have been mixed together on purpose (Townes and Holtfreter, 1955). Some cells are able to recognize their environment very specifically with their surface receptors. In an experiment in 1960s, lymphocytes were extracted from the body, radioactively labeled, and injected back to blood stream (Iwasa, Marshall and Karp, 2016). Labeling made it possible to follow their path, and it was observed that the lymphocytes returned to their sites of origin.

Adhesion proteins (sometimes called adhesion receptor proteins) on the cell surface include some members of immunoglobulin family, cadherin, integrin, selectin and mucin. Many adhesion proteins are highly specific and bind to one main ligand (Bray *et al.*, 2009; Iwasa, Marshall and Karp, 2016; Pollard, 2017). Cadherins are homophilic and bind to similar cadherins in the neighboring cells. Immunoglobulins are heterophilic and they bind other cell adhesion proteins. Selectins bind to mucins and other anionic

polysaccharides. Integrins are bit of an exception, as they can bind to fibronectin, laminin, some IgCAMs (Immunoglobulin superfamily cell adhesion molecules) and on cadherin (Pollard, 2017).

Since epithelium is in the focus of this work, cell-cell adhesion protein cadherin represents great interest. Cadherin as a name comes from calcium-dependent adhesion because the protein requires calcium ions to be present for the binding to happen (Bray *et al.*, 2009; Priest, Shafraz and Sivasankar, 2017). Cadherins have subgroups: classical cadherins, desmosomal cadherins, protocadherins and atypical cadherins, of which the classical cadherins are most studied ones. In this work the term cadherin corresponds to the classical cadherins. Cadherins are transmembrane proteins with distinct interfaces in *cis* (on the same cell) and *trans* (with different cell). Their ectodomains from opposing cells form *trans* dimers that mechanically couple cells, while their intracellular part interacts with intermediate proteins, such as catenins, that link cytoskeletal actin and cadherin together (Brasch *et al.*, 2012; Priest, Shafraz and Sivasankar, 2017). *Trans* dimers are less flexible than cadherin monomers, which pushes the adhesion forwards when adjacent cells contact each other by reducing entropic cost related to the *cis* oligomer formation (Brasch *et al.*, 2012). The *cis* clustering of cadherin i.e. their bundling on the same cell is believed to stabilize cell-cell adhesions (Brasch *et al.*, 2012; Priest, Shafraz and Sivasankar, 2017). Different regions of the ectodomains participating in the cell-cell adhesion affect the bonding type, more specifically the shape of the dimer (Leckband and de Rooij, 2014; Priest, Shafraz and Sivasankar, 2017). These different dimer shapes are named slip bonds, catch bonds and ideal bonds, reflecting their behavior under tensile stress. Slip bods, which are the most common among biomolecules, become weaker with increased tensile stress. Catch bonds strengthen when pulled, i.e. “catch” on with the pulling force. Ideal bonds’ off-rate stays constant regardless of the force amplitude (Leckband and de Rooij, 2014; Priest, Shafraz and Sivasankar, 2017). Cadherins can react to mechanical stress by switching between the dimers in single molecule tests. However, the phenomenon is yet to be proven to occur in live cells (Priest, Shafraz and Sivasankar, 2017). As stated, calcium ions are required for the proper function of cadherin. In the extracellular part of the protein there are five successive domains. Between each of them, i.e. in four locations, three calcium ions will bind. This means 12 calcium ions in total per cadherin (Boggon *et al.*, 2002). Three different effects of the calcium binding have been presented. Firstly, bound calcium ions lock in place or rigidify the characteristic crescent shape of the cadherin ectodomain (Pokutta *et al.*, 1994). Secondly, calcium helps to define the structure in “X-dimer” catch bond interfaces (Harrison *et al.*, 2010). Thirdly, it affects the “S-dimer” slip bond

energetics when opposing cadherins create the adhesions through dimerization of their subdomains (Vendome *et al.*, 2011). Cadherins are also regulated by catenin p120, which is a protein part of the intracellular cadherin-actin linkage. Catenin p120 dephosphorylation promotes cell adhesion through cadherin (Petrova, Spano and Gumbiner, 2012).

In the ECM, a glycoprotein called fibronectin provides a binding link for cells to attach. Most cells cannot attach properly on bare collagen. Other part of the fibronectin connects to collagen and the other part to the cell's integrin receptor. In humans, there are 24 different types of integrins. Integrin goes through the cell membrane and has an intracellular domain that connects to cytoskeletal actins. This provides structural support that prevents the integrin receptor from ripping off from the cell membrane. Furthermore, integrin makes it possible for a cell to move around: integrins go through conformational changes that allow them to attach to and detach from surfaces (Bray *et al.*, 2009). Integrin binding will trigger or at least facilitate different actions in cells.

Overall, cells are able to control adhesion by changing the surface density, state of aggregation and state of activation of their adhesion receptors. Considering other biomolecular interactions, ligand binding in adhesion proteins is weaker. Faster rates of binding and dissociation allow cells to move across surfaces (Pollard, 2017).

Human cancers typically have reduced cellular adhesion. This allows them to "break free" from the histological structure and order and create malignant tumors (Hirohashi and Kanai, 2004). Tumor cells can spread in the body and form metastases. This process resembles the active adhesion of leukocytes (Belloni and Tressler, 1990; Honn and Tang, 1992). After their adhesion to endothelium, cancer cells create metabolic conduits to the tumors close by. There are differences between the microvascular endothelium of tissues and organs regarding how well cancer cells can migrate through them. This is called organ preference of metastasis. It is believed to be caused by quantitative differences in the cell adhesion receptors and their bonding strength (Pauli *et al.*, 1990). Cancer spreading is not unambiguous, however, and there are parts of it open for debate. Kawaguchi, in his review about cancer metastasis and related cell adhesion molecules, supports a hypothesis where the cancer cells create microinjury to the tissues by blocking the blood flow in the capillaries which would greatly enhance their success ratio to create metastasis. This would make the adhesion properties of tumor cells less significant in their spreading to healthy tissues. In addition, in an experimental model of rat hepatoma (liver cancer) there was no proof of relationship between the substrate-adhesion potential and the ability of tumor cells to create metastases. Instead, the author

found a connection between progression of malignant tumors and the expression of carbohydrates in cancer cells (Kawaguchi, 2016). Carbohydrates bind with lectins, which are proteins who control and regulate cell adhesion and protein levels in blood (Raibon and Möller, 2009). Koch et al. reported how in 3D hydrogel traction mapping they saw invasive tumor cells taking an elongated, spindle-like shape as opposed to the spherical shape of normal cells (Koch *et al.*, 2012). They suggested that the shape change increases the traction directionality, which helps the tumor cells travel through ECM.

Cell adhesion or the lack of thereof, plays a role in few other diseases too. Leukocyte adhesion deficiency prevents white blood cells from adhering to the inner lining of blood vessels, effectively obstructing the leukocyte migration into inflamed tissue sites from occurring (Nelson, Rabb and Arnaout, 1992; Pollard, 2017). The leukocytes will also have impaired phagocytosis and aggregation. The disorder is caused by genetic mutation in two alleles which results in a structurally deformed integrin protein chain called CD18. The patients affected often suffer from severe bacterial infections that may turn out fatal (Nelson, Rabb and Arnaout, 1992). Another interesting, albeit extremely rare, disorder is Bernard-Soulier syndrome which is named after the people who first reported it in 1948 (Bernard and Soulier, 1948). The occurrence rate is only one case in a million people, as the disorder is autosomal recessive, meaning an individual would have to have gotten a faulty gene from both of the parents (Boeckelmann *et al.*, 2017). The syndrome involves defects in glycoprotein Ib-IX-V receptor complex, which serves an essential part in platelet adhesion. The receptor binds to von Willebrand factor (a blood glycoprotein that promotes hemostasis), counter receptors on activated endothelial cells or leukocytes (types of selectin and integrin), and coagulation factors, such as thrombin. Thus, the Bernard-Soulier syndrome impairs blood clotting. Those affected by the syndrome suffer from bleedings on their mucous membranes, e.g. nose or gum bleed, or prolonged bleedings after surgery or physical injury (López *et al.*, 1998; Andrews and Berndt, 2013). Bernard-Soulier syndrome has different phenotypes and the details of them are still being investigated, in hopes of finding new treatment methods. All details can be useful, of course: intracellular subunits of faulty glycoprotein Ib-IX-V receptor may have an impact on the platelet's size, and studying them has given new knowledge about normal platelet biology (Andrews and Berndt, 2013).

Khalili and Ahmad wrote a comprehensive review of different cell adhesion measurement methods for biomedical applications (Khalili and Ahmad, 2015). They describe most common techniques for single cell and cell population measurements. Different measurement techniques have been developed for specific purposes, which makes their direct comparison difficult. Rather, the researcher should pick the most suitable one

given the purpose of the tests. In this work, the single cell adhesion measurements are mostly disregarded since they do not compare to the methods used in this thesis. In summary, single cell adhesion and detachment measurements are done to investigate forces between single cells and their substrate (ECM in the body) and to observe changes cell morphology and migration. The methods are useful for obtaining very specific information about cell adhesion/detachment kinetics and the strength of the adhesions. On the downside, the techniques often require expensive and sophisticated equipment in addition to a highly skilled operator (Khalili and Ahmad, 2015). Cell population measurements do not provide as detailed information, but they represent real life tissues better e.g. in biocompatibility tests, cancer research and drug tests. Attachment measuring for cell population include tests using wash assay, resonance frequency and microfluidics. For detachment, centrifugation, spinning disk, flow chamber and microfluidics are the techniques used (Khalili and Ahmad, 2015).

Wash assay is a very simplistic method for cell attachment analysis. Cells are cultured on a surface and washed before adhesion analysis. Nonattached cells will be removed by the washing procedure before the counting. For the disadvantages, the method can be considered insensitive in comparison and requiring additional phases to acquire quantitative data (García and Gallant, 2003; Mianabadi and Yazdanparast, 2004; Park, Amin Arnaout and Gupta, 2007; Chen *et al.*, 2009).

Resonance frequency adhesion tests are based on quartz crystal microbalance acoustic wave resonator. The sensor is coated with ECM. Cells attaching to it will change wave resonator's resonant frequency. The measurement happens in real time. In addition, the piezoelectric resonator can be used as an actuator to disturb the cells (Hong *et al.*, 2006; Lord *et al.*, 2006; Marx *et al.*, 2007; Da-Silva, Soares and Ferreira, 2013).

Microfluidics can be used to measure both cell adhesion and cell detachment events. Microfluidic constructs include tissue-on-a-chip and organ-on-a-chip technologies that mimic real life tissues and organs and the blood flow in them. In adhesion tests, the cells must adhere to the substrate ligands stronger than what the hydrodynamic force of the fluid (blood) is. The constructs can be very compact in size. Fluid intake is thus low, and the flow can be accurately controlled. Although the fluid flow control may require small-scale pumps or stepper motors, the chambers can be made of polydimethylsiloxane (PDMS) with rapid prototyping. Considering the detachment events, the microscale channels ensure laminar flow that enhances shear stress on the cells. On the downside, microfluidic attachment/detachment tests are for short-term adhesions only (Lu *et al.*,

2004; Song *et al.*, 2009; Christ *et al.*, 2010; Rupprecht *et al.*, 2012; Tang *et al.*, 2012; Hartmann *et al.*, 2014).

Detachment tests can also be done with centrifugation. The force affecting cells can be controlled as function of the rotational speed of the centrifuge. Several samples can be loaded in the device at a time. As centrifuges are quite common in laboratories, the need for specialized equipment is lessened. However, counting the detached cells requires fluorescence or radiolabeling. The measurement does not happen in real time, and during a measurement, only a single force (rotational speed) can be used (Giacomello *et al.*, 1999; Reyes and García, 2003).

Spinning disk technique is similar in its principle to the centrifugation, but it is done on a disk and the rotation trajectory has a smaller diameter. Cells are cultured on the disk, and their quantity is inspected before and after with microscope. The method allows for stresses in many ranges, but it may require custom devices and is not a real time measurement (García, Ducheyne and Boettiger, 1997; Deligianni *et al.*, 2000; Michael *et al.*, 2009).

Flow chambers offer two types of test setups for cell detachment measurements: parallel and radial. A radial flow chamber consists of spherical chamber. Cells are cultured on a surface inside of it. Fluid flow is directed from the center of the chamber outwards. The chamber flow ducts have a diameter that increases the with the sphere radius, therefore decreasing the fluid flow velocity and shear stress the farther from the center the fluid flows. This allows one test to cover different detaching forces. Parallel flow chamber is simpler in its design. It has the cells on a cover slip inside a rectangular-shaped chamber. Fluid flow and shear stress are controlled with pumping system, fluid viscosity and flow chamber height. Flow chamber measurement methods provide real time cell detachment observation. Disadvantages include low detachment force and short time period of the measurements (Usami *et al.*, 1993; Vogel *et al.*, 1998; Whitney O *et al.*, 2012).

2.2 Mechanotransduction

Mechanotransduction is an essential part of cell differentiation and normal physiology. Cells are able to sense and to respond to external physical stress of varying magnitude, direction and frequencies (Discher *et al.*, 2005; Ingber, 2006). Parts of the cell associated with mechanotransduction mainly include those giving it structural support or adhesion, and the cell's nucleus containing and transcribing the genome. Focal adhesions require external forces for their maturation and growth (Geiger, Spatz and Bershadsky, 2009; Harburger and Calderwood, 2009; Yan *et al.*, 2015). Signal pathways beginning from

focal adhesions are important for cell proliferation, survival, differentiation and migration (Jaalouk and Lammerding, 2009). At the focal adhesions and cell-cell junctions, several actin binding factors in the cytoskeleton transmit the mechanical cues, throughout the cytoplasm (Sluchanko and Gusev, 2010; Zhou, Hartwig and Akyürek, 2010; Schlegelmilch *et al.*, 2011). Cytoskeleton is interconnected to the nuclear envelope via LINC (linker of nucleoskeleton and cytoskeleton) complexes, which are composed of a few proteins (Crisp *et al.*, 2006). The lamina, protein rich layer inside the nuclear envelope is mainly composed of lamin proteins (A- and B-type) and some less numerous proteins, such as lamina associated proteins 1 and 2 (LAP1 & LAP2) and emerin. A-type lamins and emerin both play a role in forwarding mechanical cues and signals from cytoplasm to nucleus (Guilluy *et al.*, 2014). Along its path inside the cell, the received cue of external force seems to affect protein conformation, localization of transcription factors, chromosome organization and the structure of the nuclear envelope, which all can influence gene expression or cell morphology.

As mentioned above, cell adhesions are essential in mechanotransduction, as they interconnect cells to their surroundings, be it other cells or extracellular matrix. Moreover, normal cells are anchorage dependent, meaning they are normally not viable if they are suspended in fluid. Cells in tissues are able to pull on their microenvironments and thus feel the stiffness of their surroundings. Their behavior can be different based on it. Growth surface stiffness influences contractility, motility and spreading of the cells. On softer surfaces, cells create less tension but they can crawl faster (Marganski, Dembo and Wang, 2003; Discher, Janmey and Wang, 2005). Swift et al. reported that culturing cells on soft surfaces resulted in round shaped cells with wrinkly nuclei, and ones cultured on stiffer gels promoted cell spreading and nuclear flattening (Swift and Discher, 2014). This knowledge can be of use in e.g. stem cell research. It appears that mimicking appropriate tissue stiffness in cell culture hydrogels is important when trying to differentiate cells towards certain types (Sweeney *et al.*, 2006; Hadden *et al.*, 2017). It has been shown that neurons prefer softer substrates (Flanagan *et al.*, 2002; Solon *et al.*, 2007) and that stem cells prefer higher stiffness (Tse and Engler, 2011; Choi *et al.*, 2012; Vincent *et al.*, 2013). In addition, mechanical and physical cues are important for adult tissue, because adult stem cells require these physical interactions with ECM to maintain their potency (Vining and Mooney, 2017).

Wallrath et al. studied the cross talk between the cytoplasm and nucleus and described the complex networks of proteins that interconnect the two together. These proteins include cell membrane receptors, cytoplasmic filaments, LINC complexes and proteins in the nuclear envelope that are connected to chromatin. Disruptions to the pathway and

cross talk lead to softening of the cytoskeleton, which can cause disease to arise in tissues that are under mechanical stress. (Wallrath, Bohnekamp and Magin, 2016) For an overview, some of the proteins involved in the cross talk are illustrated in Figure 1. From the picture, we can see how ECM and adjacent cells are able to exert forces to nucleus via the transmembrane complexes and the corresponding proteins (intermediate filaments and actin) connected to them. LINC complex, comprised of nesprin and SUN (Sad1p, UNC-84) domain proteins, can be thought to resemble focal adhesion in its function, difference being their location in the cell structure (Antoku *et al.*, 2015). Missing from the Figure 1 are the so called adherens junctions and their specific cadherin-actin linkages. LINC complexes connect the perinuclear actin cap, a cytoskeletal organelle that is made of parallel and contractile acto-myosin filament bundles, to the nucleus. The perinuclear actin cap is wrapped around the nucleus and is connected to the focal adhesions, which “completes” the pathway for some mechanical cues (Khatau *et al.*, 2009). As cells pull on their surroundings, the cytoskeleton induced stresses create equal but opposite forces to ECM and the cell nucleus (Chancellory *et al.*, 2010; Swift *et al.*, 2013; Alam *et al.*, 2015). In fact, it was discovered already in the 90s that disabling the cytoskeletal actin stress fibers makes the nucleus no longer respond to extracellular tension or compression, which indicates their essential role in mechanotransduction (Guilak, 1995; Maniotis, Chen and Ingber, 1997). Similarly, disabling the LINC complex

will lead to reduced nuclear deformation caused by external stress, implying their key role in transmitting load (Lombardi *et al.*, 2011; Driscoll *et al.*, 2015).

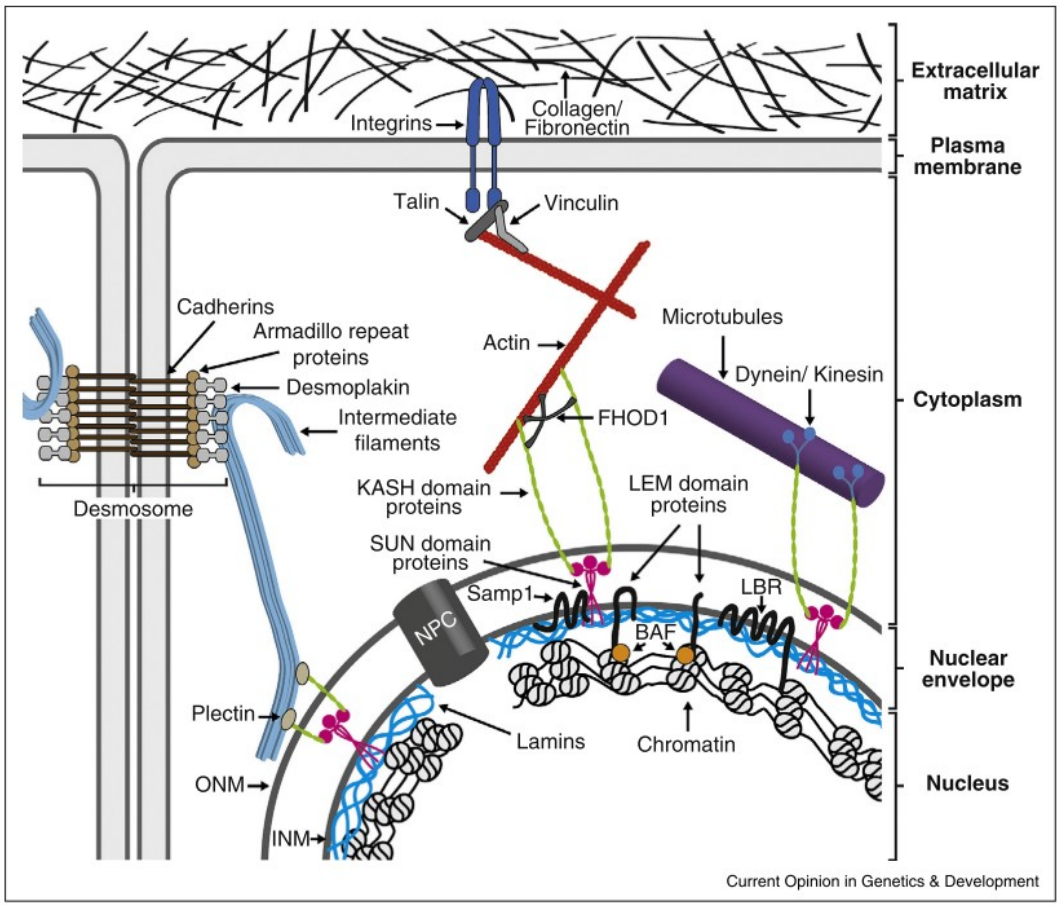

Figure 1. *A depiction of the cellular components involved in mechanocoupling nucleus to cytoplasm, plasma membrane and extra cellular matrix. The LINC complexes are formed of KASH and SUN domain proteins. Abbreviations used: KASH (Klarsicht, ANC-1, Syne Homology) domain proteins, most important here being nesprins. SUN (Sad1p, UNC-84) domain proteins, which interact with KASH proteins. FHOD1, formin homology 1/2 domain-containing protein 1. LEM, acronym of lamina-associated protein 1, emerin and MAN1. NPC, nuclear pore complex. LBR, lamin B receptor. BAF, barrier-to-autointegration factor. ONM and INM, outer/inner nuclear membrane. Image credit to Wallrath et al.* (Wallrath, Bohnekamp and Magin, 2016)

Cadherin cell-cell adhesions (i.e. adherens junctions) and their intracellular linkages to actin cytoskeleton transmit mechanical cues from outside the cell towards the nucleus, as already mentioned above. In addition, they can respond to external mechanical stress locally. Cadherin complexes involve other proteins that are important transducing mediators. Inside the cell, cadherin is bound to a protein chain consisting of β-catenin, α-catenin, vinculin and finally actin or actomyosin (see Figure 2) (Leckband and de Rooij,

2014). Through this, cadherin ligation activates signal pathway cascades that regulate cytoskeletal organization and functions such as cell differentiation and cell cycle progression (Niessen, Leckband and Yap, 2011). These pathways include Wnt/β-catenin pathway which regulates transcription (Gumbiner, 2005; Niessen, Leckband and Yap, 2011), and Hippo signaling pathway which regulates cell proliferation and apoptosis (Kim *et al.*, 2011). Cadherin complexes also transduce forces that have intracellular origin. They turn these tensions into signals that regulate certain tissue functions, such as barrier permeability and tissue remodeling (Ladoux *et al.*, 2010; Le Duc *et al.*, 2010; Liu *et al.*, 2010; Yonemura *et al.*, 2010; Leckband *et al.*, 2011). Cadherin bond types and their response to external stress was already discussed in Chapter 2.1. In living cell environment, evidence for cadherin based mechanotransduction in a local level includes force-dependent remodeling of inter-cellular junctions (Liu *et al.*, 2010); altered mechanical properties like adhesion strength and cell traction (Ladoux *et al.*, 2010; Thomas *et al.*, 2013); and junction stiffness (Le Duc *et al.*, 2010). Thomas et al. (2013) showed that adhesion between cell doublets increased after pulling them with dual micropipettes, and they concluded that it correlated with actomyosin remodeling at the cell-cell junctions (Thomas *et al.*, 2013). Leckband & Rooij (2014) state that even though through unclear feedback loops, extracellular matrix rigidity causing an increase in the internal contractile forces in cells proves that cadherin complexes are active mechanosensors (Leckband and de Rooij, 2014). In the complex sensory chain, α-catenin and vinculin are believed to have significant roles. α-catenin that links cadherin associated β-catenin to actin filaments (Desai *et al.*, 2013) (see Figure 2.) goes through a conformational change under tension which affects vinculin binding (Yonemura *et al.*, 2010). Myosin-II caused contractions (Yonemura, 2011) and external tension promote vinculin presence in cell-cell junctions (Barry *et al.*, 2014). Vinculin is hypothesized to work as a stabilizer in these junctions (Barry *et al.*, 2014). β-catenin itself does not seem to have a clear function in mechanotransduction (Leckband and de Rooij, 2014). However, free β-catenins that are not bound to cadherin can act as mediators in gene expression pathways. β-catenin binding to a transcription regulator called TCF creates a complex that promotes expression of Wnt-responsive genes, including those that stimulate cell proliferation though their products. A tumor suppressor gene named APC, that is often missing in cancer, degrades β-catenin, preventing the TCF from working (Bray *et al.*, 2009).

Plasma membrane can act as a mechanochemical transducer on its own. Mechanical stimuli can activate ion channels in the plasma membrane, of which the calcium channels are most important. Calcium ions are highly regulated within the cell and they bound to

countless proteins, affecting their localization, function and association (Clapham, 2007). Pathak et al. reported that a stretch activated calcium channel type in human neural stem cells can influence their lineage specification. Channel Piezo1 is expressed by brain derived human neural stem cells. Its activity enhances differentiation towards neural cells, and its knockdown promotes differentiation towards astrocytic lineage. Piezo1 is activated by myosin-II dependent traction forces creating tension on the cell membrane. Activation results in calcium ion influx through the membrane and nuclear localization of YAP (yes-associated protein). Although the lineage specific molecular signaling pathways are not completely understood, the finding shows one method how cellular environment affects stem cell differentiation (Pathak *et al.*, 2014). In addition, calcium channel response to stress seems to be essential for the health of cartilage in joints and the loss of this function in chondrocytes is associated with forms of arthritis (Lee *et al.*, 2014; O'Conor *et al.*, 2014). Other mechanical stress induced occurrences are the flattening of plasma membrane and promoted exocytosis (tensile stress), formation of cavities between the plasma membrane and external surface, endocytosis and clustering of membrane phospholipids (compressive stress) and plasma membrane fluidization caused by shear stress. Tension and shear forces often cause conformational changes to proteins and relocate them. These molecular changes in the membrane subsequently activate different signaling pathways, although they are still under research and not yet fully understood (Le Roux *et al.*, 2019).

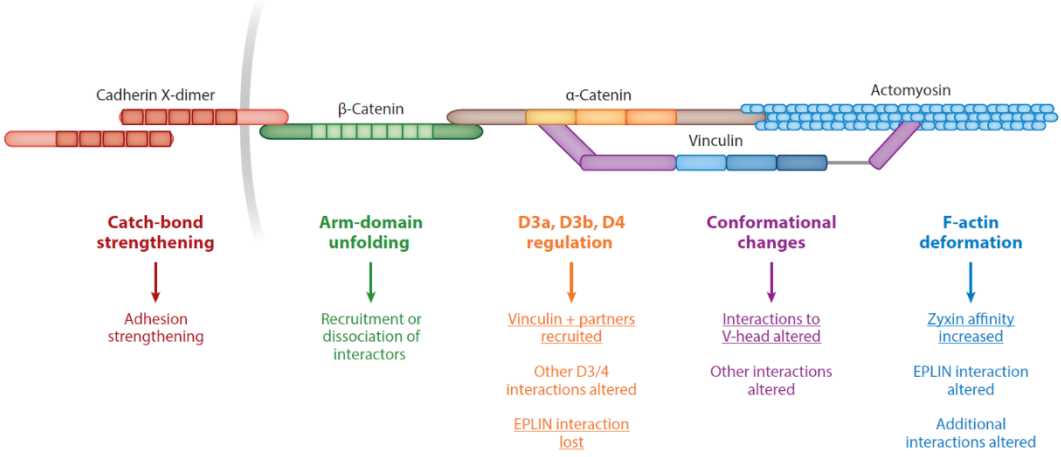

Figure 2. *Cadherin-actin complex and the properties of the parts in the sensory chain. Illustration by Leckband & Rooij (2014).*

Behavior of nuclear envelope and the nucleus in the sense of mechanotransduction are better known. With isolated nuclei, it was shown that the nucleus is mechanosensitive independent of cytoplasm (Guilluy *et al.*, 2014). As in the case of plasma membrane, proteins in nuclear envelope may undergo conformational changes that alter their

biochemical properties. Lamin A/C, which the nuclear envelope mostly comprises of, unfolds in response to mechanical tension. This change in its structure makes the protein less prone to phosphorylation which makes biochemically more stable. This means lamin A/C, and thus the nuclear envelope, have stress-strengthening properties. (Swift *et al.*, 2013) Cells on soft surfaces have more phosphorylated lamin A/C and wrinkly nuclei, and their phosphorylated lamins may become degraded (Buxboim *et al.*, 2014). However, stress-induced protein stability is not a universal phenomenon in the proteins of the cells. Collagen I of the extra cellular matrix is similar to lamin A/C in the regard of stress-strengthening (Flynn *et al.*, 2010), but for example a protein p130Cas in the cytoskeleton becomes more prone to phosphorylation once it is unfolded by external stress (Sawada *et al.*, 2006). A nuclear envelope protein called emerin will also undergo conformational changes that lead to alterations in its phosphorylation states. Contrary to lamin A/C, however, lower amount of emerin actually stiffens the nucleus. Cells growing on stiff surfaces or otherwise exposed to external stress exhibit more phosphorylation of emerin. (Guilluy *et al.*, 2014) If the phosphorylation of emerin was blocked by a mutation in critical residues of the protein, the cells would show fewer stress fibers, decreased nuclear localization of transcription coactivators YAP and TAZ (yes-associated protein and transcriptional coactivator with PDZ-binding motif, respectively), reduced migration, and lessened transcription by transcription factor SRF (serum response factor).

The external forces do not only affect the nuclear envelope and its shape. The changes are experienced inside the nucleus, too. Tension experienced by the cell affects the mobile regulators', e.g. transcription factors or transcription coactivators YAP and TAZ, passage and movement into and inside the nucleus (Halder, Dupont and Piccolo, 2012). If actin cytoskeleton induced stresses are impaired, YAP/TAZ transcription is inhibited (Dupont *et al.*, 2011). Nuclear entry of YAP and TAZ creates many signaling cascades and they affect the cell differentiation. They are localized in the nucleus in high-tension cells (Dupont *et al.*, 2011; Sun *et al.*, 2014). Another transcription factor, called NKX-2.5, goes inside the nucleus if the cell is low-tensioned and it will hold back the expression of genes that relate to high-tension states of the cell (Dingal *et al.*, 2015). Although the nuclear entry of YAP, TAZ and NKX-2.5 due to phosphorylation of nuclear envelope proteins like emerin, as previously mentioned, has been documented, it is still unclear if YAP/TAZ or NKX-2.5 directly interact with mechanosensitive proteins in the nucleus or at the nuclear envelope. (Murphy *et al.*, 2014)

In addition to the transcription factors and coactivators, external stress changes the chromatin shape and organization. Chromosome rearrangement due to external force was already discovered in 2001 (T and C, 2001). Maharana et al. reported that physical

stress alone, i.e. without biochemical agents, can alter and influence transcriptional activity. This occurs especially when the nucleus is flattened, and the chromosome territories become mingled and intertwined with each other (Maharana *et al.*, 2016). Lamins in the inner nuclear envelope bind LADs (lamina associated domains) of the chromatin and tethers heterochromatin to the outer region or the “edges” of the nucleus. This region is also called the nuclear periphery and highly packed heterochromatin is usually found there. Heterochromatin contains silent genes and it is compact in its form. It is thought this binding of heterochromatin to lamina is associated with repressed gene expression (Guelen *et al.*, 2008; Wilson and Foisner, 2010). Supporting this claim is the fact that gene expression is influenced by the spatial arrangement of the DNA sequences inside the chromosomes (Misteli, 2007; Sexton *et al.*, 2007; Hübner and Spector, 2010; Bickmore and Van Steensel, 2013) and that the genes located at the periphery of the nucleus, i.e. close to the lamin membrane and LADs, are suppressed. Illustration of this is presented in Figure 3. If the gene sections are opened and brought inwards to the nucleus, their transcription is increased (Ragoczy *et al.*, 2006; Szczerbal, Foster and Bridger, 2009; Peric-Hupkes *et al.*, 2010; Yao *et al.*, 2011; Demmerle, Koch and Holaska, 2013; Lund *et al.*, 2013; Dobrzynska *et al.*, 2016). Artificially stretching a chromatin fiber has shown that a 5 pN force is needed to decondense a 30 nm long fibre (Cui and Bustamante, 2000). Such forces can be induced by the microtubule polymerization (Hampoelz *et al.*, 2011). Furthermore, observing a labeled chromatin and creating localized tension with magnets on the cell surface showed that the gene transcription elevated, albeit the chromatin being a non-native/endogenous (Tajik *et al.*, 2016). On a similar note, forces of same range (i.e. piconewtons) can also change histone acetylation states (Li *et al.*, 2011) and interactions between proteins inside the nucleus (Poh *et al.*, 2012). Chromatin wraps around the histones, and Li et al. discovered that in mesenchymal stem cells external strain changes histone acetylation state, namely promoting the acetylated form and possibly altering chromatin remodeling. Another interesting discovery relating to reorganization of chromatin is the nuclear compression induced structural polarization of lamin A/C in basal-to-apical direction, which may explain the positioning and conformation changes of chromosome domains under stress (Ihalainen *et al.*, 2015).

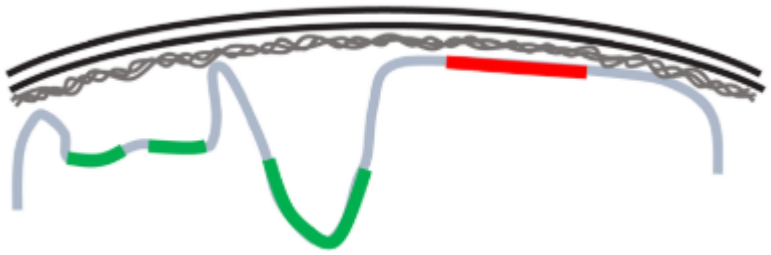

Figure 3. A *section of a chromatin partially attached to nuclear envelope and lamins. Silent gene, here colored as red, is bound to the lamina and the actively transcribed genes (green) are located towards the nuclear interior. Image credit to Szczensy & Mauck.* (Szczesny and Mauck, 2016)

In most of the publications of the subject, mechanotransduction has been approached as something that might explain changes in nuclear shape and gene expression in differentiating or mature cells. However, there are researchers who do not share this point of view, at least to certain extent. Li et al. stated that nuclear deformation is mostly based on the cell spread area, and individual components like the perinuclear actin cap and LINC complexes do not affect it that much (Li *et al.*, 2015). In their review article about cell nucleus' stand in mechanotransduction the authors Szczesny and Mauck say that based on the research papers the effects of mechanotransduction and outside forces may have been overstated. The forces arising from inside the cytoskeleton and cell spread area contribute the most to the nuclear shape, with outside stress having a smaller effect (Szczesny and Mauck, 2016). Furthermore, there are arguments that conformational changes in lamin A/C and the reorganization of chromatin are mainly a method to protect the genetic information from being damaged, rather than a mean to alter gene expression. As established, the lamin A/C forms the main structural support of the nuclear envelope. The nuclear lamina remodels itself and goes through conformational changes that stabilize, and thus strengthen, its structural integrity, preventing outside forces creating damage to the envelope (Swift *et al.*, 2013; Buxboim *et al.*, 2014; Kim, Cho and Wirtz, 2014; Swift and Discher, 2014; Machowska, Piekarowicz and Rzepecki, 2015). If lamin A/C is absent, the cells go through major nuclear and chromatin conformation deformations under external stress (Lammerding *et al.*, 2004; Neelam *et al.*, 2015; Makhija, Jokhun and Shivashankar, 2016). Zwerger et al. reported that laminopathies (mutations regarding lamin coding genes), that cause disease in muscle tissue, made the cell nuclei deformed and impaired the coupling between nucleus and cytoskeleton. Laminopathies that did not cause muscular dystrophy also did not decrease the stiffness of the nucleus, which may imply that

weakened nuclei suffer from genetic damage in tissues under stress and tension, such as muscle (M. *et al.*, 2013). In addition to the nuclear envelope's responsivity to stress, the significance of chromatin location in the nucleus and the role of LADs in gene expression is not wholly agreed upon. There is evidence that a gene is silenced before it is moved to the nuclear periphery, meaning that the location alone does not determine the state of transcriptional activity for it (Brown *et al.*, 1999; Reddy *et al.*, 2008). Likewise, taking genes from the nuclear lamina and moving them to the inner region of the nucleus does not always activate them and they keep silent (Gartenberg *et al.*, 2004). On some occasions being located and even associated with nuclear lamina does not suppress the gene, which further leads to believe that the genetic activity is more complex and dependent of several factors (Sexton *et al.*, 2007; Hübner and Spector, 2010).

In their review article about nuclear mechanosensing the authors Cho, Irianto and Discher summarize some of the research explaining the origins of diseases related to nuclear mechanosensing. Impaired functionality of nuclear mechanosensory proteins is linked to diseases impeding the normal development of an infant. They mostly affect bone, cardiac, cartilage and muscle tissues. Disorders associated with this are, for example, dilated cardiomyopathy (weakened cardiac contractility, thinned ventricular walls) and muscular dystrophy (Cho, Irianto and Discher, 2017). Initially the nuclei are soft and feeble in the non-differentiated embryonic cells (Pajerowski *et al.*, 2007). Lamin A/C expression is increased after the tissue differentiates. In mice, failure to express lamin A/C leads to suppressed growth and eventual death due to degeneration of cardiac, adipose, and muscle tissue (Kubben *et al.*, 2011; Jahn *et al.*, 2012). Kubben et al. reported that their mice lacking LMNA, the lamin A/C coding gene, only lived two to three weeks after being born due to their severely underdeveloped hearts and metabolic complications. In Hutchinson-Gilford progeria syndrome, which is a rare syndrome that causes premature aging in humans, a mutation in LMNA makes the lamin A/C unable to effectively rearrange under mechanical stress (Dahl *et al.*, 2006). This causes the nucleus to become stiffer, brittle and more fragile than in a healthy cell.

2.3 Epithelium

Epithelial cells form sheets that line all external and internal surfaces in the body. They protect the organs from external hazards such as pathogens, prevent fluid loss and regulate transition of chemicals in and out of the organs. Many epithelial tissues also serve a function of secretion of e.g. sweat or hormones. Epithelium has several different cell junctions that connect it to the extracellular matrix and the cells within itself together. The junctions can serve as pathways for chemical signaling, provide strength in the layer

of cells or prevent molecules from passing between the cells (Freshney and Freshney, 2002; Bray *et al.*, 2009; Iwasa, Marshall and Karp, 2016).

Tight junctions seal neighboring cells with each other and prevent leaking of the epithelium, i.e. anything going through between the epithelial cells. Tight junctions are essential for absorptive cells lining the inside of the intestines to prevent diffusion of the absorbed molecules to the "wrong" direction. Tight junctions have comparatively complex protein composition, as they consist of at least 40 different proteins. Most important ones are the claudin family of proteins, occludin, and junctional adhesion molecules (JAMs) that are part of the immunoglobulin superfamily (Anderson and Van Itallie, 2009). The claudins are believed to be the defining part in tight junctions' sealing functionality (Anderson and Van Itallie, 2009) whereas occludin is more of a regulator (Saitou *et al.*, 2000). Saitou et al. (2000) reported that nulling the occludin gene did not affect the tight junctions in mice, but it resulted in reduced postnatal growth and many tissue defects, such as calcification of the brain and thinning of the compact bone (Saitou *et al.*, 2000). Similarly, JAMs serve as regulators in tight junction formation during the acquisition of cell polarity that some cells represent (e.g. basal-to-apical epithelial cells, nerve cells) (Ebnet, 2004).

Gap junctions are important for cell-cell communication since they create channels between the cells. They allow inorganic ions and small hydrophilic molecules to pass from cytosol to cytosol (Bray *et al.*, 2009; Iwasa, Marshall and Karp, 2016). Gap junctions in vertebrae are comprised of integral membrane proteins called connexins. Six connexins form a connexon. Two connexons, both from adjacent cells, dock together and create the gap junction (Goodenough, 1996; Sáez *et al.*, 2003).

Junctions holding the cells together include adherens junctions, desmosomes and hemidesmosomes. Epithelial cells have cadherin proteins on their surface, which connect to those of the adjacent cells. An adherens junction is a protein complex, where a cadherin molecule goes through the cell membrane and is attached to cytoskeletal actin filaments via linker proteins, as already discussed in Chapter 2.1. The extracellular part will bind with cadherin from another cell. Adherens junctions often form a continuous belt of connections between the epithelial cells, close to the cells' apical end. This interconnection of cells via actin bundles and cadherin complexes of the adherens junctions allow epithelium to create tension and to change its shape. Tight junctions are located above adherens junctions. In a desmosome, different cadherin molecules connect bundles of keratin filaments in adjacent cells. Desmosomes have very high tensile strength and they are prevalent in skin. Hemidesmosomes are similar in structure.

They connect epithelial cells from their basal surface to the connective tissue. Proteins creating the connection are transmembrane integrins that are linked to intracellular keratin filaments (Bray *et al.*, 2009; Iwasa, Marshall and Karp, 2016).

Epithelial cells are known for their renewability (Freshney and Freshney, 2002; Bray *et al.*, 2009). In biotechnology, they are used for studying the regulation of cell proliferation and differentiation. Epithelial cells show higher rate of malignant transformations likely due to their fast pace of regeneration, which is why they are also used in cancer research (Freshney and Freshney, 2002). Epithelium represents the source of cancer in 90% of the cases (Frank, 2018). Typical cells isolated from normal tissue can only proliferate for a limited number of division cycles. Through mutation or bioengineering a cell line can become immortal and divide without a limit. These cell lines are useful in scientific purposes. Immortal epithelial cell lines include dog kidney epithelium (Madin-Darby Canine Kidney, MDCK), mink lung epithelium (“Mv1 Lu”) and epithelium from monkey kidney (“BS-C-1”).

2.4 Piezoelectric effect

Piezoelectric effect is herein addressed shortly, since in this work it’s used as a tool and is not in the focus of the essential research. Direct piezoelectric effect is observed in certain materials, where an external stress or strain creates a polarization of charges within the material. The polarization is proportional to the stress applied, and it creates an electric field across the material. Converse piezoelectric effect means an external electric field causing strain or stress to the piezoelectric material, which in practice is observed as deformations in its shape (Jiang *et al.*, 2017; Topolov, Bowen and Bisegna, 2018a).

Piezoelectric materials usually have dielectric crystalline structures. Commercially, they are used for example in actuators, transformers, accelerometers and strain gauges. Piezo sensitivity varies by the material. Composites are used in modern piezoelectric solutions to achieve piezoactivity together with other desirable features (Topolov, Bowen and Bisegna, 2018a).

Piezoelectric effects and piezoactive materials have their established mathematical models which are well defined in literature, for example by Topolov, Bowen and Bisegna (2018) (Topolov, Bowen and Bisegna, 2018b).

3 MATERIALS AND METHODS

3.1 Cell vibration system

Desired function for the constructed stimulation system was to provide horizontal motion to the cells with known acceleration values, while maintaining the possibility to view the cells with a microscope simultaneously. The device was designed to fit into the microscope sample holder and to not physically interfere with the optics. Chassis dimensions are 127 x 86 x 10 mm. Movement is generated with two disc-shaped piezo elements.

The device consists of three major parts: chassis, piezo disks and piezo-moved sample holder with the accelerometer (Figure 4). Chassis and sample holder are made of 3D-printed (Original Prusa i3 Mk2, Prusa Research a.s., Prague, Czech Republic) PLA (polylactic acid) filament (3DPrima, Prima Printer Nordic AB, Malmö, Sweden). 3D-printing allows for quick prototyping and ease of design with computer software (SolidWorks 2018, Dassault Systèmes SolidWorks Corporation, Waltham, Massachusetts USA), which were preferred in this project since optimization of the device design required iteration. PLA is lightweight and affordable polymer. Since there were no additional requirements for e.g. exceptional tensile strength or permeability, it was a suitable choice for the material. However, in this work the mechanical properties and interference or effect to the resonant frequency were not studied in comparison to other materials. Sample holder is attached non-permanently to the chassis with the piezo discs, which means the construction can be taken apart. More specifically, the sample

holder rests on the piezo disks that themselves have mounting slots in the frame. Therefore, no adhesives or screws are required.

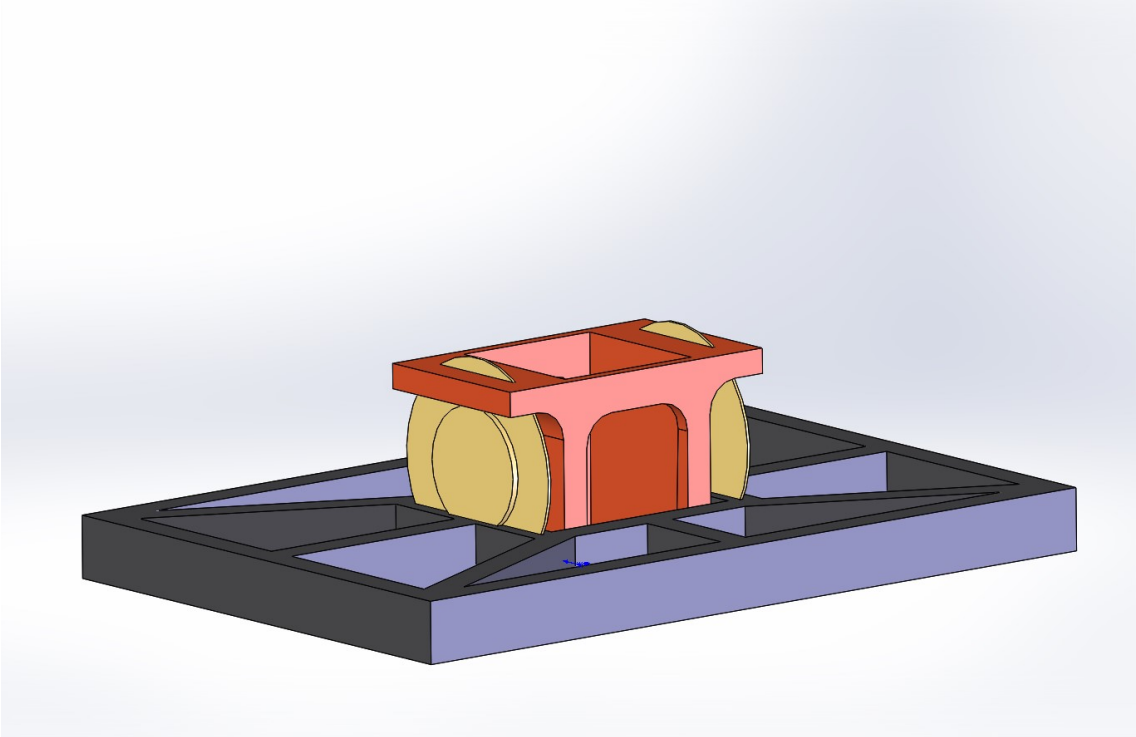

Figure 4. *A computer rendering of the shaker device. Bottom section (grey) is the frame, yellow spherical objects are the piezo disks and the red structure on top is the sample holder.*

The piezo discs are made of lead zirconate titanate (PZT) ceramic. As per converse piezoelectric effect, PZT will deform physically as a function of externally supplied voltage. The discs are assembled in a way that voltage causes them to bend, which can be observed as a difference in horizontal distance between the top and the bottom of the vertically placed disc. This bending creates the horizontal movement to the sample holder. Piezo elements were chosen because they have a high bandwidth, they are lightweight, affordable and compact in size (PI Ceramic GmbH, 2014). In addition, they come in different sizes and specifications and the design of the shaker device allows for them to be switched, if necessary. The piezo discs used in this work were acquired from Farnell and manufactured by Multicomp. They are 35 mm in diameter with a resonance frequency of 2800 MHz and maximum voltage of 30 Vpp (Multicomp, 2014). They were driven with a signal generator (Keysight 33210A, Keysight Technologies, USA).

Cells are cultured inside a polydimethylsiloxane (PDMS, Sylgard 184, Dow Corning, USA) well resting on a square glass slide (Figure 5). The well is 1 ml in volume and together with the glass side 14 mm tall. These wells are handmade by casting PDMS in a mold, and attaching it to the glass. The mold was 3D-printed from PLA. After casting, the PDMS was cured at 60 °C for 10 hours and removed from the mold. To ensure vertical optical transparency, the middle section of the well bottom was removed with a 6 mm diameter biopsy punch. The PDMS well was then attached on 22 mm x 22 mm microscopy glass slide on which it adhered by itself. The completed PDMS-glass

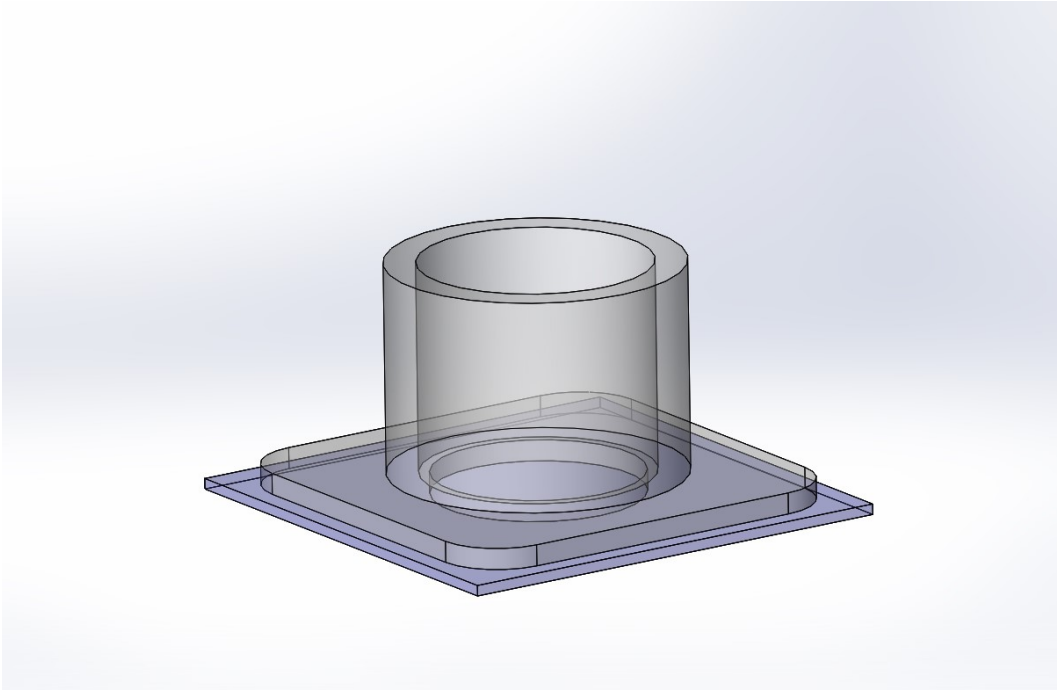

Figure 5. *A computer rendering of the PDMS well resting on square glass slide.*

construct holds liquid and is transparent. The well is loaded to the sample holder from the top side.

The sample holder also mounts the accelerometer. Wiring from the piezos and accelerometer is routed to the front of the device to a small circuit board that also houses the connectors for Arduino and a signal generator.

Initial data processing from the accelerometer was done with an Arduino Due board. Arduino boards are simplistic electronic platforms that are extensible, affordable and open source. The software to run them is open source as well and the programming interface software is available for all operating systems (Arduino, 2019b). Arduino has many different types of boards of which the Due model represents one of the more powerful and connectable ones (Arduino, 2019a). However, the Due was chosen since it was at hand at the time and not because the project required it. Same functionality

could have been achieved with the smaller and somewhat less capable One model, which was first considered as the board of choice. Arduino Due has a 32-bit ARM processor and it can be connected to a PC with USB-cable. It has 54 digital input/output connectors that can output 3,3 volts (Arduino, 2017).

Accelerometer used in the shaker device is model ADXL345 manufactured by Analog Devices (Massachusetts, USA) and it was acquired from Farnell. It is a 3-axis accelerometer with a resolution of 13 bits and measurement range up to ±16 *g*. It only uses 40 µA in measurement mode with a typical supply voltage of 2,5 V, which makes it so low power it can be easily powered by any Arduino board. In addition, the compact size of 3 mm x 5 mm x 1 mm and small weight of 20 mg were considered favorable features for the accelerometer given the measures of the shaker device. The code to run ADXL345 with Arduino is available on the Appendix A and the rough working protocol is presented in Figure 5. It was created using the help of SparkFun ADXL345 library that is licensed as Creative Commons BY-SA 4.0. Acceleration readings are provided as milli-Gs, and the output can be viewed either visually or numerically inside the Arduino software. Proper acceleration values were calculated with MATLAB software (MATLAB R2018a, MathWorks, Natick, Massachusetts USA) by taking the raw numeric acceleration value output and filtering the background noise and then calculating the mean value. Filtering was done with peak detection function and thresholding the peaks above the noise. The code also has a function to create piezo impulses should the piezos be connected to the Arduino board. However, as previously mentioned, Arduino Due cannot output more than 3,3 volts from the connectors. This voltage is not enough to create significant movement with the piezo elements so the piezo functionality of the code was mainly for testing purposes.

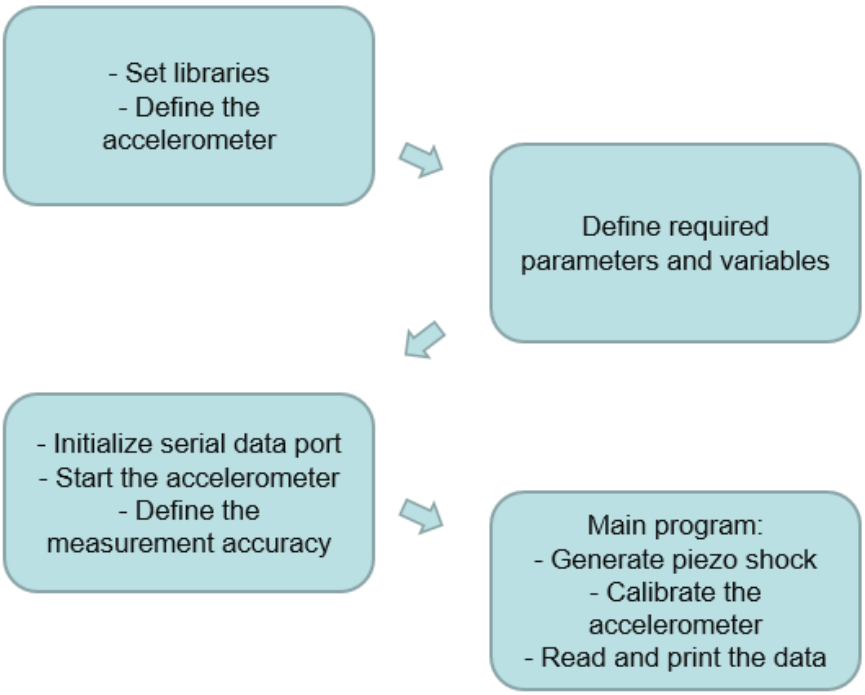

Figure 5. *ADXL345 acceleration data acquisition program structure.*

3.2 Cell culturing, microscopy and testing methods

Madin-Darby Canine Kidney (MDCK) type II cells were maintained in low glucose minimal essential medium (MEM, #41090093, Thermo Fisher Scientific, Gibco™, Paisley, UK) supplemented with 1% (vol/vol) penicillin-streptomycin antibiotics (#15140122, Thermo Fisher Scientific, Gibco™, Paisley, UK) and with 10% fetal bovine serum (#10500064, Thermo Fisher Scientific, Gibco™, Paisley, UK). For the experiments, MDCK cells were trypsinized and seeded on collagen I (#A1064401, Thermo Fisher Scientific, Gibco™, Paisley, UK) coated cover glasses (22 mm x 22 mm, high performance, D=0.17 mm, Carl Zeiss Microscopy, NY, USA) with a PDMS well seven days before imaging. Prior to imaging, the media was replaced with fresh MEM and supplemented with 25 mM HEPES buffer (#15630056, 1M, Thermo Fisher Scientific, Gibco™, Paisley, UK). Cells were imaged on a Zeiss LSM780 (ZEISS, Oberkochen, Germany) inverted laser scanning confocal microscope with a heated incubation unit using a 60x water objective (numerical aperture = 1.2).

The square wave with a frequency of 70 Hz and amplitude of 10 Vpp was deemed fit for the tests. It resulted in about 1,35 *g* mean acceleration peaks. Two test consisted of two test samples and two control samples each. Vibration system was installed in Zeiss LSM

780 confocal microscope's sample tray. MDCK cell cultures inside their PDMS well were carefully inserted in the vibration device sample holder, directly on top of the lens. Heated incubation unit was on throughout the testing phase. A short preliminary vibration was done to ensure the PDMS sample sat properly in the holder (and the image focus was not distorted) and that the piezo discs were connected to the signal generator. Test samples were subjected to the vibration for 30 minutes, with visual checking in the beginning and at the end to ensure the cells were being vibrated. During the second test the effect of recovery time before fixing was assessed: the test had recovery times of one hour for one cell culture and two hours for the other.

The samples were then fixed, one in methanol and the other in paraformaldehyde, immunolabeled and imaged. Methanol fixed samples were stained for beta-catenin (cadherin binding partner) and Alexa-647 linked secondary antibody. Nuclei and chromatin were stained with DAPI (4',6-Diamidino-2-Phenylindole) to be visible at 405 nm wavelenght. Cell-cell adhesions were stained with Occludin-Emerald and were visible at 488 nm wavelenght. Samples fixed in paraformaldehyde had DAPI and Occluding-Emerald stains similarly. Actin was stained with Phalloidin 565 and excited with 546 nm wavelenght laser. YAP was labeled with Alexa Fluor 647, visible with 633 nm laser. Control samples were fixed and labelled with the same reagents and imaged. Imaging was done with Nikon A1+ confocal microscope (Nikon, Tokyo, Japan) (N.A. = 1.4). Images were acquired as 16-bit and 1024 by 1024 pixels. YAP analysis was made with ImageJ Fiji software (v1.52p, Wayne Rasband, National Institutes of Health, USA). YAP intensity analysis was done to determine if YAP localized to nucleus or cytoplasm. Nucleus and cytoplasm DAPI channels were converted to a mask and inverted, and YAP intensity was measured from 5 fields. Since the wanted result was the intensity ratio between nuclear and cytoplasmic YAP, the intensities were not normalized to the mean intensity of the whole image.

4 RESULTS

Initially the cell vibration tests were planned to be done with sinusoidal voltage with a frequency close to the resonant frequency of the piezo elements. Testing the sinusoidal voltage frequencies showed that the piezo disks would not generate sufficient movement below 700 Hz. Even though the acceleration values could be obtained with the ADXL345 at high frequency sinusoidal voltage, it turned out during observation under the

microscope that the PDMS well mounted on the glass would slip inside the sample holder. In other words, the sample holder was moving but the cells were not. To address this issue, the voltage waveform was changed to square wave and a small layer of PDMS was added on the sample holder to provide more friction between PLA and glass. Observing the sample with the microscope, a suitable square wave frequency was determined based on the movement of the sample and whether or not the sample would stay in focus. Frequency evaluation started from 1 Hz, where there was not enough movement. At 1 kHz the PDMS well would jump out of focus and indicate lack of friction. Same thing would occur at 210 Hz albeit not as quickly. Because the samples would seize following the movement at those frequencies, they were not used in the vibration experiments. Acceleration values of the tested frequencies are presented in Figure 6.

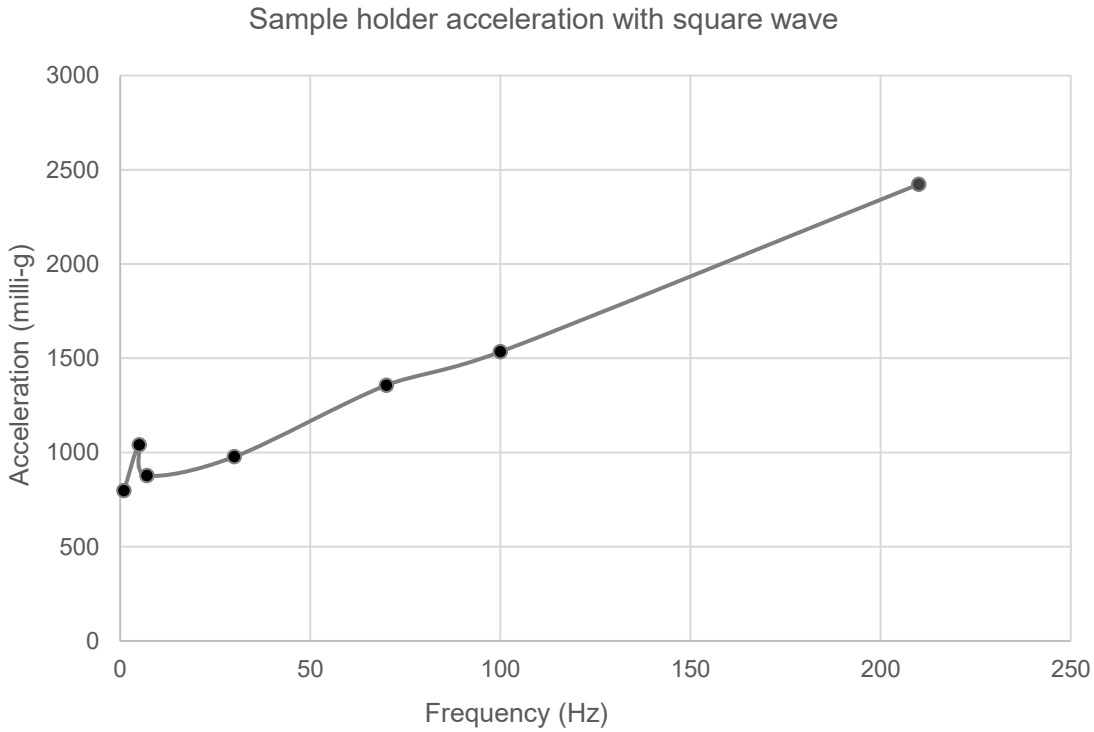

Figure 6. *Peak acceleration at the sample holder measured with square wave voltage of 10 Vpp.*

Microscopy pictures from the first experiment are summarized in Figures 7 and 8. Figure 7 contains the images of samples fixed with methanol (MetOH). Figure 8 contains images from cells fixed with paraformaldehyde (PFA). In both figures, lamin A/C and occludin intensities look higher in test samples versus the controls. Actin and β-catenin have no such visual differences.

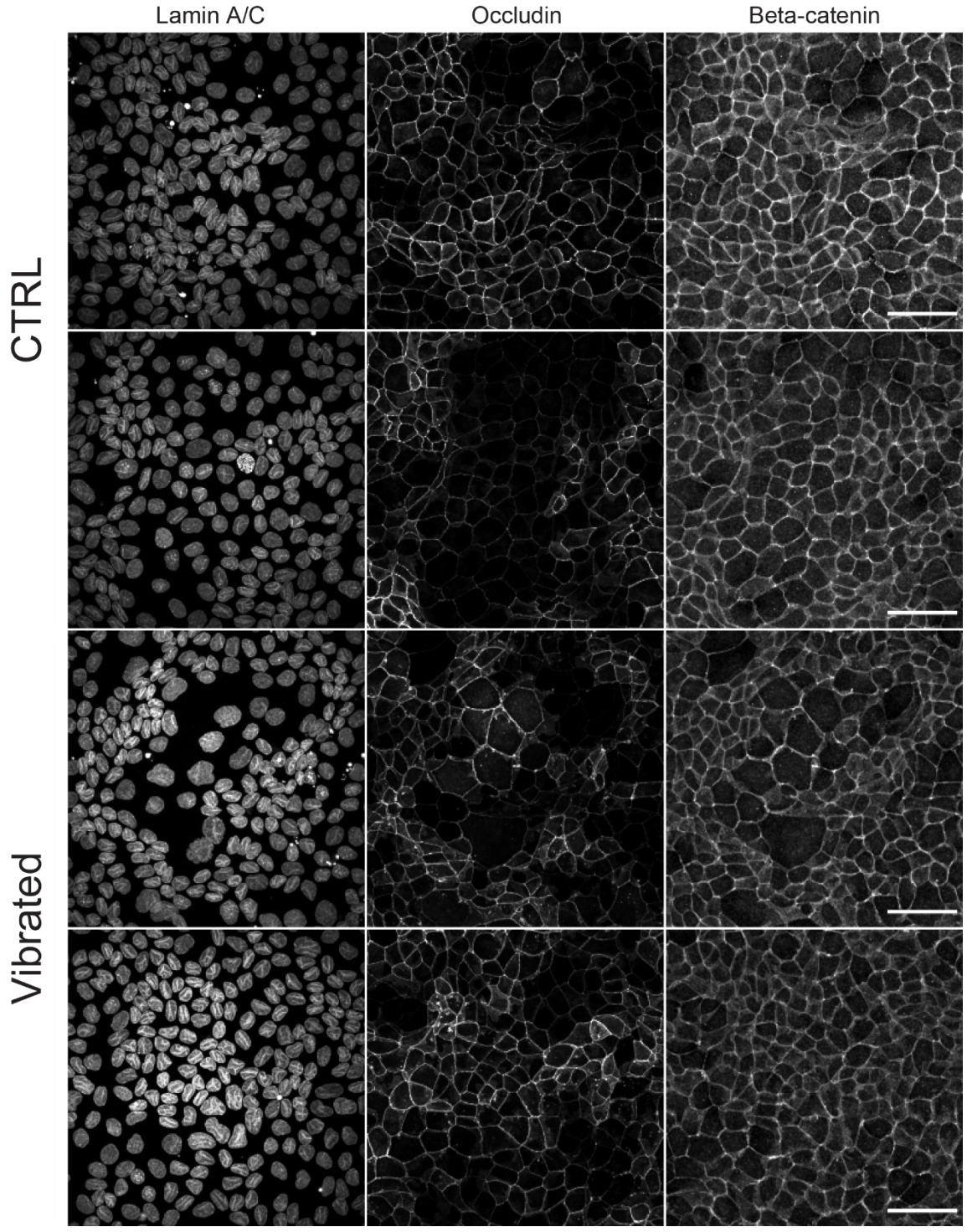

Figure 7. *Summarization of pictures taken from MetOH fixed samples. Scale bars are 50 µm.*

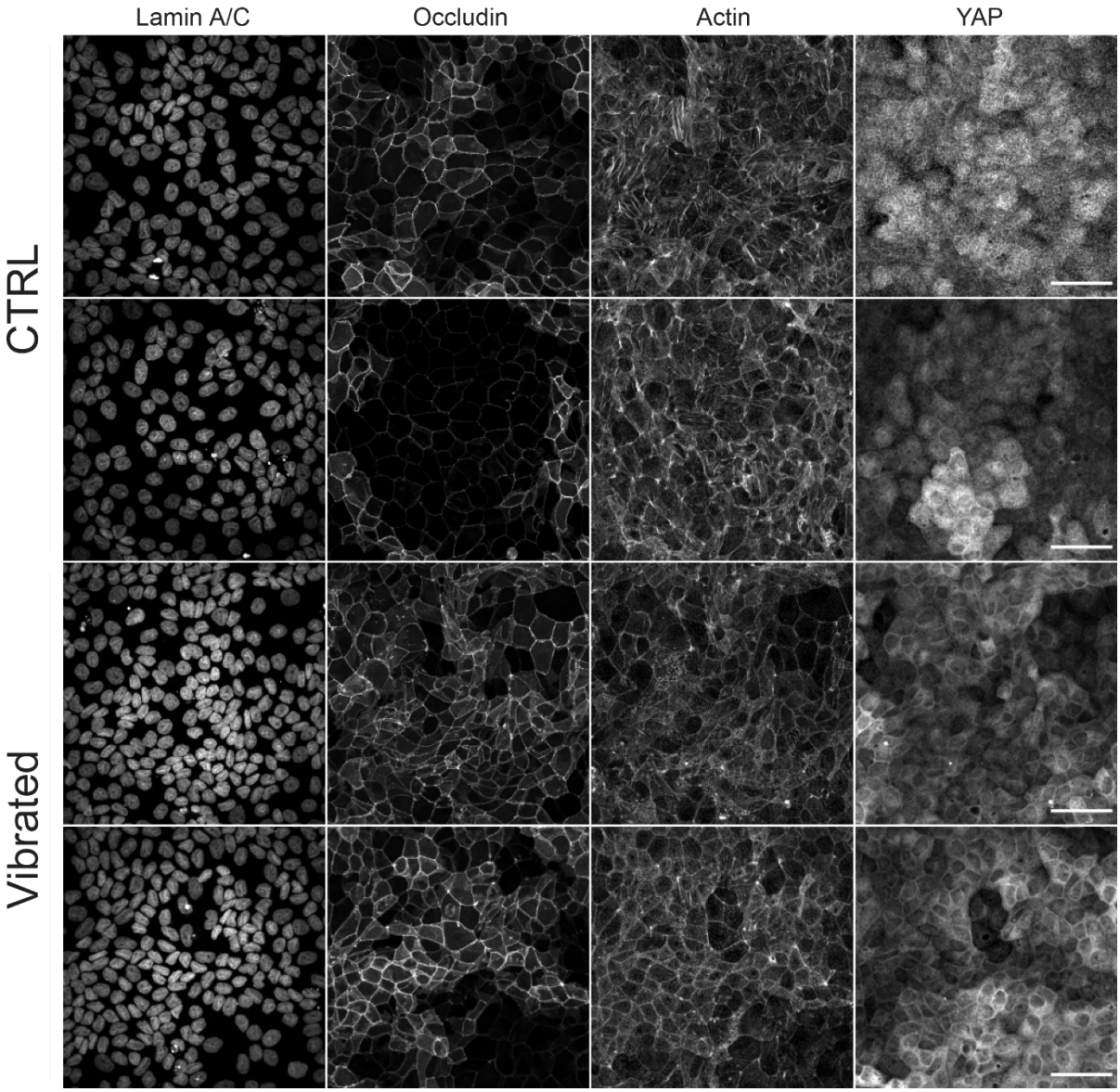

Figure 8. *Summarization of pictures taken of samples fixed in PFA. Scale bars are 50 µm.*

For better detail and easier comparison, occludin-tagged images are presented in Figures 9 and 10. Occludin is a protein found in tight junctions. Control samples had larger areas in the middle of the cell culture, where cell-cell junctions were seemingly lower in numbers.

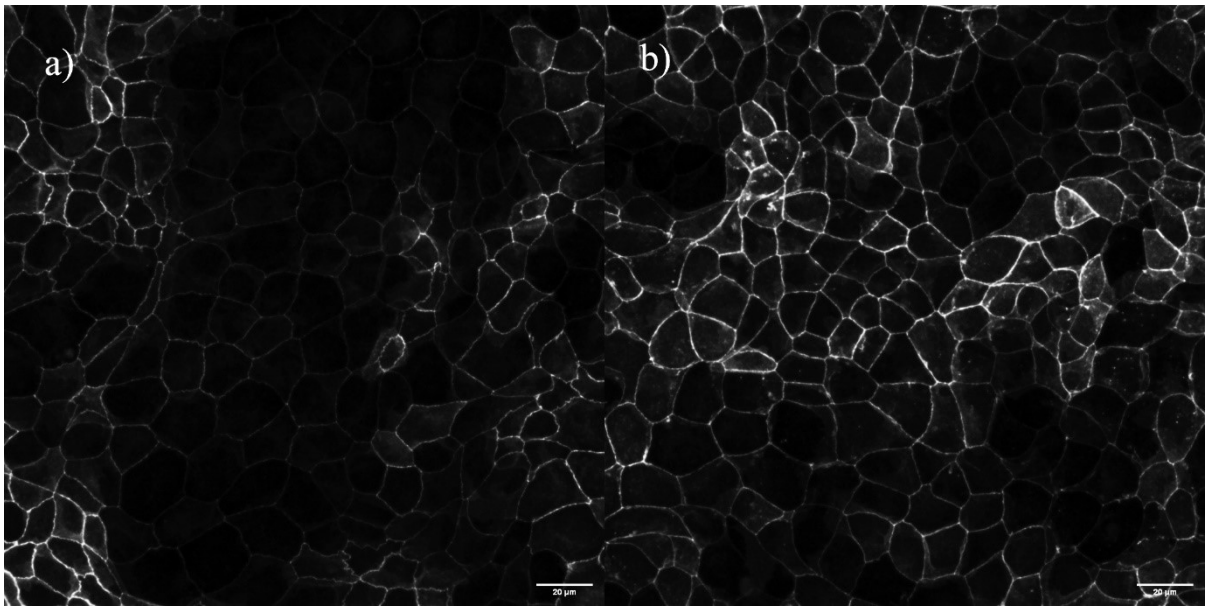

Figure 9. *Side-by-side image of stained control sample a) and test sample b) both fixed with MetOH.. Scale bars are 20 µm. Noticeable is the increased intensity of labelled occludin in the middle section of the test sample, which also emphasizes the cell outlines.*

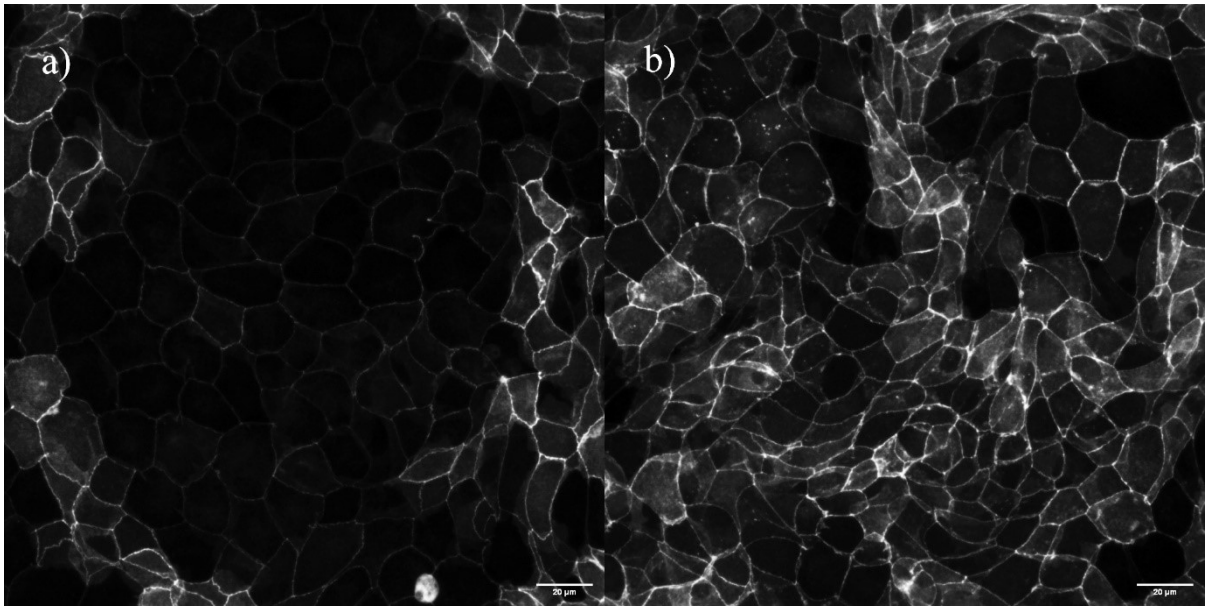

Figure 10. *Side-by-side image of stained control sample a) and test sample b) both fixed in PFA. Scale bars are 20 µm. Occludin stains are clearly more visible in the test sample on cell outlines, where tight junctions are located.*

In visual inspection, YAP localization seemed to have changed more towards the cytoplasm. In Figure 8 and in greater detail in Figure 11, stained YAP looks to be located

in nuclei in the control sample cells. Vibrated test samples do not have such great intensities in the middle of the cells. Instead the labelled YAP seems to fill the entire cells, emphasizing their outlines.

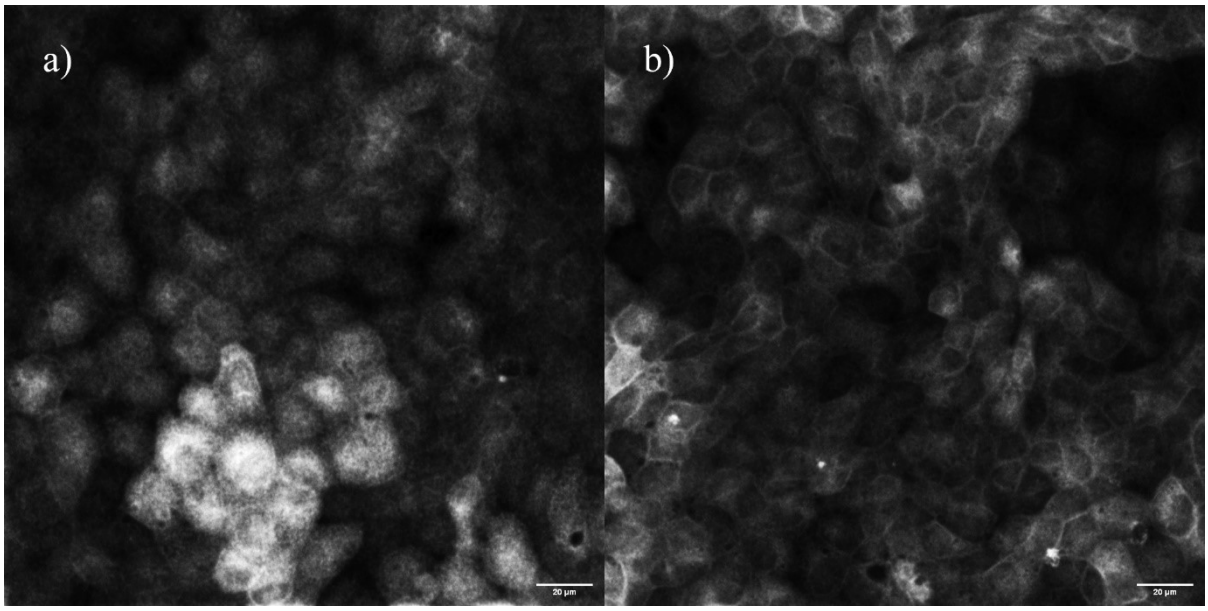

Figure 11. *Control cell culture a) and the vibrated cells b) with labeled YAP.*

In the second experiment, different recovery times before the fixing were compared. Despite the visually perceived YAP relocalization in the first experiment, further analysis showed there was, in fact, no meaningful changes in it. In addition, nuclear shape had no significant changes. Table 1 has the summarized results of the YAP intensity analysis. Intensity values listed in Table 1 are unitless, and their range depends on the bit depth of the images (here, the images were 16-bit). However, the most important data is the ratio between nucleoplasmic and cytoplasmic intensities. Full details can be found in Appendix B.

Table 1. *YAP analysis on samples with recovery times of one hour and two hours. There were no significant changes in YAP relocalization.*

Sample recovery time	Area of interest	Nucleoplasmic intensity	Cytoplasmic intensity	NP/CP ratio
Control	Middle	92,4	96,2	0,966
1h	Middle	94,7	92,6	1,03
	Edge	103,1	96,6	1,07
2h	Middle	85,4	88,8	0,965
	Edge	85,9	89,4	0,964

Visual differences between the control sample and test samples in the second experiment were scarce compared to the first run. DNA was stained with DAPI to better see nuclei shape. A collage of the microscope pictures is presented in Figure 12.

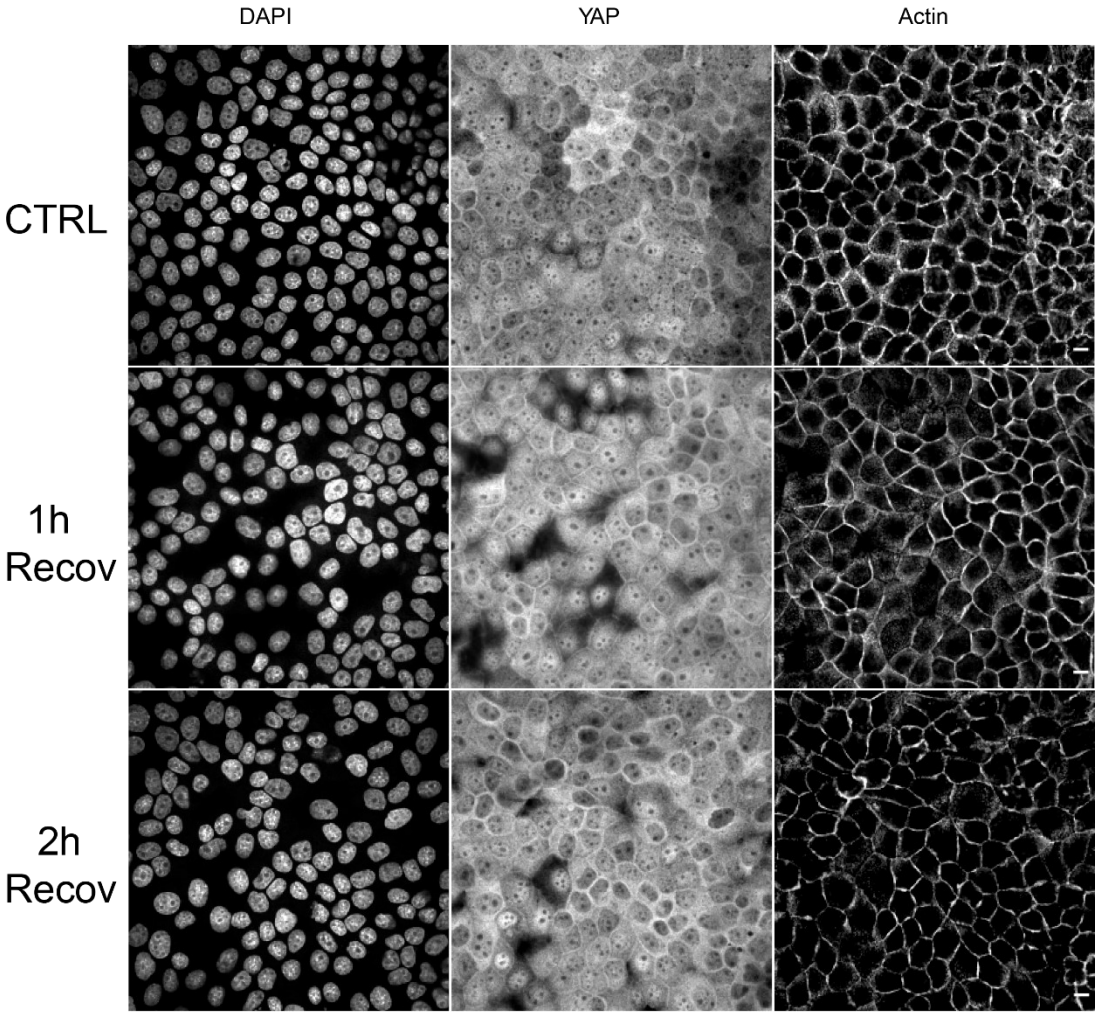

Figure 12. *Comparison between different recovery times after the second vibration experiment. No meaningful variations are present. DAPI labels regions in DNA. Scale bars are 50 µm.*

5 DISCUSSION

We can see from the microscope picture collages (Figures 7 and 8) that the most distinguishable differences between control samples and the vibrated test samples occur with lamin A/C and occludin expression. Vibrated cells have higher intensity in these

labelled proteins, making them stand out better in the pictures. Labelled lamin A/C brings more contrast to the nuclei areas. Occludin emphasizes the cell outlines very well in the vibrated cells, whereas the control samples have areas with very low occludin intensity that appear dark. As explained earlier, lamin A/C is an important component of the nuclear lamina, and occludin is a protein that is involved in the structure of tight junctions. These results fit in with the hypothesis on how the cells would respond to the external physical stress. Ostensibly the cells have strengthened the nucleus and have adhered to their surroundings more tightly.

Unexpectedly however, there were no meaningful differences in nuclei shape or YAP localization, even though it initially looked like it would be the case. In Figure 11, YAP seems to localize into the cytoplasm after vibration, but similar effect does not occur in Figure 12. Furthermore, actin or β-catenin intensities did not noticeably increase. There may be a connection between the absence of change in actin and YAP localization. Dupont et al. (2011) state that YAP/TAZ respond to the tension in actin cytoskeleton stiffness independently from Hippo signaling pathway (Dupont *et al.*, 2011). Vibration created by the system here does not result in continuous tension. In addition, the acceleration may not be high enough to stress the cytoskeleton thoroughly, which is something that could be tested with some modifications to the system, namely with larger piezo discs and higher driving voltage. YAP/TAZ are also regulated by Hippo signaling pathway and their phosphorylation states vary based on the pathway activity. Inactivation of Hippo pathway results in dephosphorylation of YAP/TAZ and their accumulation (and activity as transcription regulators) in nucleus (Halder, Dupont and Piccolo, 2012). In order to find out what exactly happens with YAP/TAZ, their phosphorylation instances should somehow be monitored.

Moreover, one might ask why does occludin intensity have a clear difference between control and test samples, while β-catenin does not? They are both involved in cell-cell adhesions, after all. As discussed in Chapter 2.1, β-catenin is part of adherens junction and occludin is related to tight junction protein complexes. This points to a conclusion that tight junctions respond to the mechanical stimulus more so than adherens junctions; however, such claim is not backed by literature. Instead, more repeats of cell vibration tests would be needed, possibly with different staining or cell culturing methods.

There is no exactly similar approach to mechanotransduction and cell adhesion research as used in this work. In other publications, the frequencies vary from around 1-200 Hz (Gaston *et al.*, 2012; Zhang *et al.*, 2012; Kanie *et al.*, 2019) to kilohertz range (Tsimbouri *et al.*, 2017). Grasland-Mongrain et al. (2018) used 15 kHz frequency; however, their

intention was not to observe how the cells would respond biologically but rather to demonstrate a mean to measure cell elasticity (Grasland-Mongrain *et al.*, 2018). Not all publications have the data about the acceleration values involved. It is more common to provide the range of motion. Moving the cells is approached differently in the research papers. There are bioreactors built for long term testing (Gaston *et al.*, 2012; Tsimbouri *et al.*, 2017) and repurposed devices used as tools to have precise movement, including speaker element (Tirkkonen *et al.*, 2011) or industrial vibration calibrator (Kanie *et al.*, 2019).

In a design point of view, the shaker device used in this work is very compact in size and rather simplistic in a sense that in only creates horizontal movement. It also does not hold many cells nor medium for them. For comparison, the bioreactor presented by Gaston et al. (2012) holds two cell seeded substrates and provides vibration and strain to the samples as well as tilting powered by stepper motors (Gaston *et al.*, 2012). On the other hand, while not matching the complexity of Gaston's bioreactor, our device is able to fit in the microscope tray which is a novel feature in itself. Moreover, many of the other publications aimed to study stem cell differentiation, which was not the case in this thesis work. Tsimbouri (2017), Tirkkonen (2011) and Zhang (2012) were specifically interested in osteogenetic differentiation. This work required the cells to be cultivated and kept alive for longer periods than during the testing performed as part of this thesis. Curiously, all the aforementioned authors stated that the vibration did successfully promote stem cells to differentiate towards bone-forming cells (Tirkkonen *et al.*, 2011; Zhang *et al.*, 2012; Tsimbouri *et al.*, 2017).

Tsimbouri et al. (2017) used piezo elements to create the movement in their bioreactor. The range of motion was 15 – 30 nm. The authors speculate that motion in the range of 20 nm could be helpful in diverting stem cells towards osteogenic lineage (Tsimbouri *et al.*, 2017), based on the findings on how stem cells respond to nanotopographical features of their surroundings (Dalby, Gadegaard and Oreffo, 2014). In our case, the range of motion was not available from the piezo element datasheet. We could visually estimate the movement to be couple of times the diameter of MDCK samples i.e. in the range of tens of micrometers. In this thesis, the motion range was not considered other than vaguely it having to be adequate. If the research interest would be in the stem cell differentiation, the piezo elements should be selected more carefully, using the publications about cell nanotopography as guidance.

As previously stated, the frequency and amplitude used in this thesis work were 70 Hz in square form and 10 Vpp, respectively. Mean peak acceleration was about 1,35 G with

those settings. Kanie et al. (2019) used a slightly similar frequency and acceleration setting, which they described as “tapping” in 1 or 200 Hz frequency. Acceleration was reported to be 1 or 2 G; the values were most likely made available by the industrial vibration calibrator they used to create the movement. However, their system provided vertical movement unlike our cell shaker device. The experiments were done to induced pluripotent stem cells. Kanie et al. wanted to simulate how common occurrences related to cell laboratories, such as closing of the incubator door or dropping something on a tabletop, would affect stem cell growth. The acceleration values were sufficient to induce changes in the cells after enough passages: Kanie et al. state that the vibrations can enhance cell growth in the beginning, but the tapping can create shear stress that dissociates the cells and the growth profile and cell adhesion would be eventually negatively affected (Kanie *et al.*, 2019).

It is unfortunate that the acceleration values are not commonly measured in the mechanotransduction themed research, making precise comparison with our results difficult. While the focus in mechanotransduction research is seemingly skewed towards stem cell differentiation, observing the effects on matured tissues could provide useful information for tissue engineering. For instance, Gaston et al. (2012) studied how vocal fold fibroblasts and stromal stem cells responded to vibration and compared the expression levels of certain genes in them. In their discussion, they make a good point how the vibration frequency could have been chosen better to represent the human male voice range too (Gaston *et al.*, 2012). On the other hand, their comparison between stem cells and differentiated tissue cells is quite novel. They also referred to a previous publication by Titze (1989) reporting 1 kHz frequencies and over 200 *g* accelerations that vocal fold mucosa is subjected to (Titze, 1989), establishing an upper limit of sort for the testing. With our shaker device, using cells from different tissues and having piezo elements of variable sizes could provide very useful information from a tissue engineering point of view.

6 CONCLUSIONS AND FUTURE ASPECTS

In this thesis work the goal was to see how epithelial cells would respond to horizontal vibration created by a custom built, affordable cell shaker device. 30 minutes of vibration to the cells created more cell-to-cell adhesions (tight junctions) as seen from increased occludin expression levels. However, cell nuclei and YAP localization did not change

significantly, although it first seemed like it in visual inspection. Actin and β-catenin responses were also minimal, at least visually. This lack of clear changes in the inner parts of the cells leaves room for improving the testing methodology used in this work. The most obvious things to reconsider are the vibration time and acceleration. Both of them could be increased, for example placing the vibration system inside an incubator unit and raising the voltage driving the piezo discs.

In the light of the results, this thesis works more as a presentation of new research method. The shaker device itself performed in most admissible fashion. It is unfortunate that the intended sine wave frequencies were not usable, but on the other hand, the square waveform proved to be adequate considering the results obtained. Compared to other devices used in publications related to similar research, this shaker device is very affordable and simplistic in its design and construct. The possibility for simultaneous microscopical imaging, sample vibration and acquisition of acceleration values are novel.

For the future development, it would be reasonably straight forward to duplicate or build several of vibration systems with slight differences in the piezo element size and thus in the sample holder dimensions too. All of the components needed for the system are inexpensive. With multiple systems it would be possible to have a larger range of frequencies and ranges of motion available for testing. It would open vast possibilities for the research of cell adhesion and mechanotransduction. One could test the response of a specific cell line to different accelerations or frequencies, or alternatively use a number of devices with the same specifications to test and compare the response of different cell types at a set frequency. Other purposes for the shaker device come from the ability to observe the sample in real time. One possible usage could be evaluating changes in cell adhesion and viability under slight movement to changes in cell medium, for example pH or ion concentrations. Going even further, the shaker device design could be entirely re-done to create more axes of movement by including more piezo elements and changing their angles. With digital controllers such as the Arduino, the piezos could “fire” periodically and provide e.g. a vortical movement for the sample.

REFERENCES

Alam, S. G. *et al.* (2015) 'The nucleus is an intracellular propagator of tensile forces in NIH 3T3 fibroblasts', *Journal of Cell Science*, 128(10), pp. 1901–1911. doi: 10.1242/jcs.161703.

American Physical Therapy Association. (2001) 'Guide to Physical Therapist Practice. Second Edition. American Physical Therapy Association.', *Physical therapy*, 81(1), pp. 9–746. Available at: http://www.ncbi.nlm.nih.gov/pubmed/11175682.

Anderson, J. M. and Van Itallie, C. M. (2009) 'Physiology and Function of the Tight Junction', *Cold Spring Harbor Perspectives in Biology*, 1(2), pp. a002584–a002584. doi: 10.1101/cshperspect.a002584.

Andrews, R. and Berndt, M. (2013) 'Bernard-Soulier Syndrome: An Update', *Seminars in Thrombosis and Hemostasis*, 39(06), pp. 656–662. doi: 10.1055/s-0033-1353390.

Antoku, S. *et al.* (2015) 'Reinforcing the LINC complex connection to actin filaments: The role of FHOD1 in TAN line formation and nuclear movement', *Cell Cycle*, 14(14), pp. 2200–2205. doi: 10.1080/15384101.2015.1053665.

Arduino (2017) *Getting started with the Arduino Due*. Available at: https://www.arduino.cc/en/Guide/ArduinoDue (Accessed: 4 September 2019).

Arduino (2019a) *Arduino Products*. Available at: https://www.arduino.cc/en/Main/Products (Accessed: 4 September 2019).

Arduino (2019b) *Frequently Asked Questions*. Available at: https://www.arduino.cc/en/Main/FAQ (Accessed: 4 September 2019).

Ayad, N. M. E., Kaushik, S. and Weaver, V. M. (2019) 'Tissue mechanics, an important regulator of development and disease', *Philosophical Transactions of the Royal Society B: Biological Sciences*, 374(1779), p. 20180215. doi: 10.1098/rstb.2018.0215.

Barry, A. K. *et al.* (2014) ' -Catenin cytomechanics - role in cadherin-dependent adhesion and mechanotransduction', *Development*, 141(10), pp. e1006–e1006. doi: 10.1242/dev.111419.

Bauer, M. S. *et al.* (2019) 'Structural and mechanistic insights into mechanoactivation of focal adhesion kinase.', *Proceedings of the National Academy of Sciences of the United States of America*, 116(14), pp. 6766–6774. doi: 10.1073/pnas.1820567116.

Belloni, P. N. and Tressler, R. J. (1990) 'Microvascular endothelial cell heterogeneity: Interactions with leukocytes and tumor cells', *Cancer and Metastasis Review*, 8(4), pp. 353–389. doi: 10.1007/BF00052608.

Bernard, J. and Soulier, J. P. (1948) 'Sur une nouvelle variété de dystrophie thrombocytairehémoṛragipare congénitale.', *La semaine des hopitaux : organe fonde par l'Association d'enseignement medical des hopitaux de Paris*, 24(Spec. No.), pp. 3217–23. Available at: http://www.ncbi.nlm.nih.gov/pubmed/18116504.

Bickmore, W. A. and Van Steensel, B. (2013) 'Genome architecture: Domain organization of interphase chromosomes', *Cell*, 152(6), pp. 1270–1284. doi: 10.1016/j.cell.2013.02.001.

Boeckelmann, D. *et al.* (2017) 'Patients with Bernard-Soulier syndrome and different severity of the bleeding phenotype.', *Blood cells, molecules & diseases*, 67, pp. 69–74.

doi: 10.1016/j.bcmd.2017.01.010.

Boggon, T. J. *et al.* (2002) 'C-cadherin ectodomain structure and implications for cell adhesion mechanisms', *Science*, 296(5571), pp. 1308–1313. doi: 10.1126/science.1071559.

Brasch, J. *et al.* (2012) 'Thinking outside the cell: how cadherins drive adhesion', *Trends in Cell Biology*, 22(6), pp. 299–310. doi: 10.1016/j.tcb.2012.03.004.

Bray, A. *et al.* (2009) *Essential Cell Biology, 4th edition*. Garland Science. doi: citeulike-article-id:4505949.

Brown, K. E. *et al.* (1999) 'Dynamic repositioning of genes in the nucleus of lymphocytes preparing for cell division', *Molecular Cell*, 3(2), pp. 207–217. doi: 10.1016/S1097-2765(00)80311-1.

Burridge, K., Monaghan-Benson, E. and Graham, D. M. (2019) 'Mechanotransduction: from the cell surface to the nucleus via RhoA', *Philosophical Transactions of the Royal Society B: Biological Sciences*, 374(1779), p. 20180229. doi: 10.1098/rstb.2018.0229.

Buxboim, A. *et al.* (2014) 'Matrix elasticity regulates lamin-A,C phosphorylation and turnover with feedback to actomyosin', *Current Biology*, 24(16), pp. 1909–1917. doi: 10.1016/j.cub.2014.07.001.

Chancellory, T. J. *et al.* (2010) 'Actomyosin tension exerted on the nucleus through nesprin-1 connections influences endothelial cell adhesion, migration, and cyclic strain-induced reorientation', *Biophysical Journal*, 99(1), pp. 115–123. doi: 10.1016/j.bpj.2010.04.011.

Chen, Y. *et al.* (2009) 'Combined Integrin phosphoproteomic analyses and small interfering RNA-based functional screening identify key regulators for cancer cell adhesion and migration', *Cancer Research*, 69(8), pp. 3713–3720. doi: 10.1158/0008-5472.CAN-08-2515.

Cho, S., Irianto, J. and Discher, D. E. (2017) 'Mechanosensing by the nucleus: From pathways to scaling relationships', *Journal of Cell Biology*, 216(2), pp. 305–315. doi: 10.1083/jcb.201610042.

Choi, Y. S. *et al.* (2012) 'The alignment and fusion assembly of adipose-derived stem cells on mechanically patterned matrices', *Biomaterials*, 33(29), pp. 6943–6951. doi: 10.1016/j.biomaterials.2012.06.057.

Christ, K. V. *et al.* (2010) 'Measurement of single-cell adhesion strength using a microfluidic assay', *Biomedical Microdevices*, 12(3), pp. 443–455. doi: 10.1007/s10544-010-9401-x.

Clapham, D. E. (2007) 'Calcium Signaling', *Cell*, 131(6), pp. 1047–1058. doi: 10.1016/j.cell.2007.11.028.

Crisp, M. *et al.* (2006) 'Coupling of the nucleus and cytoplasm: Role of the LINC complex', *Journal of Cell Biology*, 172(1), pp. 41–53. doi: 10.1083/jcb.200509124.

Cui, Y. and Bustamante, C. (2000) 'Pulling a single chromatin fiber reveals the forces that maintain its higher-order structure', *Proceedings of the National Academy of Sciences of the United States of America*, 97(1), pp. 127–132. doi: 10.1073/pnas.97.1.127.

Da-Silva, A. C., Soares, S. S. and Ferreira, G. N. M. (2013) 'Acoustic detection of cell adhesion to a coated quartz crystal microbalance - implications for studying the biocompatibility of polymers', *Biotechnology Journal*, 8(6), pp. 690–698. doi:

10.1002/biot.201200320.

Dahl, K. N. *et al.* (2006) 'Distinct structural and mechanical properties of the nuclear lamina in Hutchinson-Gilford progeria syndrome', *Proceedings of the National Academy of Sciences of the United States of America*, 103(27), pp. 10271–10276. doi: 10.1073/pnas.0601058103.

Dahl, K. N., Ribeiro, A. J. S. and Lammerding, J. (2008) 'Nuclear shape, mechanics, and mechanotransduction', *Circulation Research*, 102(11), pp. 1307–1318. doi: 10.1161/CIRCRESAHA.108.173989.

Dalby, M. J., Gadegaard, N. and Oreffo, R. O. C. (2014) 'Harnessing nanotopography and integrin-matrix interactions to influence stem cell fate', *Nature Materials*, 13(6), pp. 558–569. doi: 10.1038/nmat3980.

Deligianni, D. D. *et al.* (2000) 'Effect of surface roughness of hydroxyapatite on human bone marrow cell adhesion, proliferation, differentiation and detachment strength', *Biomaterials*, 22(1), pp. 87–96. doi: 10.1016/S0142-9612(00)00174-5.

Demmerle, J., Koch, A. J. and Holaska, J. M. (2013) 'Emerin and histone deacetylase 3 (HDAC3) cooperatively regulate expression and nuclear positions of MyoD, Myf5, and Pax7 genes during myogenesis', *Chromosome Research*, 21(8), pp. 765–779. doi: 10.1007/s10577-013-9381-9.

Desai, R. *et al.* (2013) 'Monomeric α-catenin links cadherin to the actin cytoskeleton', *Nature Cell Biology*, 15(3), pp. 261–273. doi: 10.1038/ncb2685.

Dingal, P. C. D. P. *et al.* (2015) 'Fractal heterogeneity in minimal matrix models of scars modulates stiff-niche stem-cell responses via nuclear exit of a mechanorepressor', *Nature Materials*, 14(9), pp. 951–960. doi: 10.1038/nmat4350.

Discher, D. E. ; *et al.* (2005) *Tissue Cells Feel and Respond to the Stiffness of Their Substrate*.

Discher, D. E., Janmey, P. and Wang, Y. L. (2005) 'Tissue cells feel and respond to the stiffness of their substrate', *Science*, 310(5751), pp. 1139–1143. doi: 10.1126/science.1116995.

Dobrzynska, A. *et al.* (2016) 'The nuclear lamina in health and disease', *Nucleus*, 7(3), pp. 233–248. doi: 10.1080/19491034.2016.1183848.

Drinkwater, B. L. (1994) 'Does physical activity play a role in preventing osteoporosis?', *Research Quarterly for Exercise and Sport*, 65(3), pp. 197–206. doi: 10.1080/02701367.1994.10607620.

Driscoll, T. P. *et al.* (2015) 'Cytoskeletal to Nuclear Strain Transfer Regulates YAP Signaling in Mesenchymal Stem Cells', *Biophysical Journal*, 108(12), pp. 2783–2793. doi: 10.1016/j.bpj.2015.05.010.

Le Duc, Q. *et al.* (2010) 'Vinculin potentiates E-cadherin mechanosensing and is recruited to actin-anchored sites within adherens junctions in a myosin II-dependent manner', *Journal of Cell Biology*, 189(7), pp. 1107–1115. doi: 10.1083/jcb.201001149.

Dupont, S. *et al.* (2011) 'Role of YAP/TAZ in mechanotransduction', *Nature*, 474(7350), pp. 179–184. doi: 10.1038/nature10137.

Ebnet, K. (2004) 'Junctional adhesion molecules (JAMs): more molecules with dual functions?', *Journal of Cell Science*, 117(1), pp. 19–29. doi: 10.1242/jcs.00930.

Flanagan, L. A. *et al.* (2002) 'Neurite branching on deformable substrates', *NeuroReport*, 13(18), pp. 2411–2415. doi: 10.1097/00001756-200212200-00007.

Flynn, B. P. *et al.* (2010) 'Mechanical strain stabilizes reconstituted collagen fibrils against enzymatic degradation by mammalian collagenase matrix metalloproteinase 8 (MMP-8)', *PLoS ONE*, 5(8). doi: 10.1371/journal.pone.0012337.

Frank, S. A. (2018) 'Dynamics of Cancer', *Dynamics of Cancer*. Princeton University Press, pp. 59–82. doi: 10.2307/j.ctv301gwh.

Freshney, R. I. and Freshney, M. G. (eds) (2002) *Culture of Epithelial Cells*. New York, USA: John Wiley & Sons, Inc. (Culture of Specialized Cells). doi: 10.1002/0471221201.

García, A. J., Ducheyne, P. and Boettiger, D. (1997) 'Quantification of cell adhesion using a spinning disc device and application to surface-reactive materials', *Biomaterials*, 18(16), pp. 1091–1098. doi: 10.1016/S0142-9612(97)00042-2.

García, A. J. and Gallant, N. D. (2003) 'Stick and grip: Measurement systems and quantitative analyses of integrin-mediated cell adhesion strength', *Cell Biochemistry and Biophysics*, 39(1), pp. 61–73. doi: 10.1385/CBB:39:1:61.

Gartenberg, M. R. *et al.* (2004) 'Sir-mediated repression can occur independently of chromosomal and subnuclear contexts', *Cell*, 119(7), pp. 955–967. doi: 10.1016/j.cell.2004.11.008.

Gaston, J. *et al.* (2012) 'The response of vocal fold fibroblasts and mesenchymal stromal cells to vibration', *PLoS ONE*, 7(2). doi: 10.1371/journal.pone.0030965.

Geiger, B., Spatz, J. P. and Bershadsky, A. D. (2009) 'Environmental sensing through focal adhesions', *Nature Reviews Molecular Cell Biology*, 10(1), pp. 21–33. doi: 10.1038/nrm2593.

Giacomello, E. *et al.* (1999) 'Centrifugal assay for fluorescence-based cell adhesion adapted to the analysis of ex vivo cells and capable of determining relative binding strengths', *BioTechniques*, 26(4), pp. 758–766. doi: 10.2144/99264pf01.

Glatt, V., Evans, C. H. and Stoddart, M. J. (2019) 'Regenerative rehabilitation: The role of mechanotransduction in orthopaedic regenerative medicine', *Journal of Orthopaedic Research*, 37(6), pp. 1263–1269. doi: 10.1002/jor.24205.

Goodenough, D. A. (1996) 'Connexins, Connexons, and Intercellular Communication', *Annual Review of Biochemistry*, 65(1), pp. 475–502. doi: 10.1146/annurev.biochem.65.1.475.

Grasland-Mongrain, P. *et al.* (2018) 'Ultrafast imaging of cell elasticity with optical microelastography', *Proceedings of the National Academy of Sciences of the United States of America*, 115(5), pp. 861–866. doi: 10.1073/pnas.1713395115.

Guelen, L. *et al.* (2008) 'Domain organization of human chromosomes revealed by mapping of nuclear lamina interactions', *Nature*, 453(7197), pp. 948–951. doi: 10.1038/nature06947.

Guilak, F. (1995) 'Compression-induced changes in the shape and volume of the chondrocyte nucleus', *Journal of Biomechanics*, 28(12), pp. 1529–1541. doi: 10.1016/0021-9290(95)00100-X.

Guilluy, C. *et al.* (2014) 'Isolated nuclei adapt to force and reveal a mechanotransduction pathway in the nucleus', *Nature Cell Biology*, 16(4), pp. 376–381. doi: 10.1038/ncb2927.

Gumbiner, B. M. (2005) 'Regulation of cadherin-mediated adhesion in morphogenesis', *Nature Reviews Molecular Cell Biology*, 6(8), pp. 622–634. doi: 10.1038/nrm1699.

Hadden, W. J. *et al.* (2017) 'Stem cell migration and mechanotransduction on linear

stiffness gradient hydrogels', *Proceedings of the National Academy of Sciences of the United States of America*. National Academy of Sciences, 114(22), pp. 5647–5652. doi: 10.1073/pnas.1618239114.

Halder, G., Dupont, S. and Piccolo, S. (2012) 'Transduction of mechanical and cytoskeletal cues by YAP and TAZ', *Nature Reviews Molecular Cell Biology*, 13(9), pp. 591–600. doi: 10.1038/nrm3416.

Hampoelz, B. *et al.* (2011) 'Microtubule-induced nuclear envelope fluctuations control chromatin dynamics in Drosophila embryos', *Development*, 138(16), pp. 3377–3386. doi: 10.1242/dev.065706.

Harburger, D. S. and Calderwood, D. A. (2009) 'Integrin signalling at a glance', *Journal of Cell Science*, 122(2), pp. 159–163. doi: 10.1242/jcs.018093.

Harrison, O. J. *et al.* (2010) 'Two-step adhesive binding by classical cadherins', *Nature Structural and Molecular Biology*, 17(3), pp. 348–357. doi: 10.1038/nsmb.1784.

Hartmann, A. *et al.* (2014) 'A novel tool for dynamic cell adhesion studies-the De-Adhesion Number Investigator DANI', *Lab on a Chip*, 14(3), pp. 542–546. doi: 10.1039/c3lc50916h.

Hirohashi, S. and Kanai, Y. (2004) 'Cell adhesion system and human cancer morphogenesis', *Gann Monographs on Cancer Research*, 52, pp. 13–26. doi: 10.1111/j.1349-7006.2003.tb01485.x.

Hong, S. *et al.* (2006) 'Real-time analysis of cell-surface adhesive interactions using thickness shear mode resonator', *Biomaterials*, 27(34), pp. 5813–5820. doi: 10.1016/j.biomaterials.2006.07.031.

Honn, K. V. and Tang, D. G. (1992) 'Adhesion molecules and tumor cell interaction with endothelium and subendothelial matrix', *Cancer and Metastasis Reviews*, 11(3–4), pp. 353–375. doi: 10.1007/BF01307187.

Hornberger, T. A. *et al.* (2005) 'Intracellular signaling specificity in response to uniaxial vs. multiaxial stretch: implications for mechanotransduction', *American Journal of Physiology-Cell Physiology*, 288(1), pp. C185–C194. doi: 10.1152/ajpcell.00207.2004.

Huang, C. *et al.* (2013) 'Biological effects of cellular stretch on human dermal fibroblasts', *Journal of Plastic, Reconstructive & Aesthetic Surgery*, 66(12), pp. e351–e361. doi: 10.1016/j.bjps.2013.08.002.

Hübner, M. R. and Spector, D. L. (2010) 'Chromatin dynamics.', *Annual review of biophysics*, 39, pp. 471–89. doi: 10.1146/annurev.biophys.093008.131348.

Hynes, R. 0 (1992) *Integrins: Versatility, Modulation, and Signaling in Cell Adhesion Review*, *Cell*.

Ihalainen, T. O. *et al.* (2015) 'Differential basal-to-apical accessibility of lamin A/C epitopes in the nuclear lamina regulated by changes in cytoskeletal tension', *Nature Materials*, 14(12), pp. 1252–1261. doi: 10.1038/nmat4389.

Ingber, D. E. (2006) 'Cellular mechanotransduction: Putting all the pieces together again', *FASEB Journal*, 20(7), pp. 811–827. doi: 10.1096/fj.05-5424rev.

Iwasa, J., Marshall, W. F. and Karp, G. (2016) *Karp's cell and molecular biology : concepts and experiments*. 8th edn. John Wiley & Sons.

Jaalouk, D. E. and Lammerding, J. (2009) 'Mechanotransduction gone awry', *Nature Reviews Molecular Cell Biology*, 10(1), pp. 63–73. doi: 10.1038/nrm2597.

Jahn, D. *et al.* (2012) ‘ A truncated lamin A in the Lmna −/− mouse line ’, *Nucleus*, 3(5), pp. 463–474. doi: 10.4161/nucl.21676.

Jiang, X. *et al.* (2017) *High Frequency Piezo-Composite Micromachined Ultrasound Transducer Array Technology for Biomedical Imaging*. ASME Press. doi: 10.1115/1.860441.

Joshi, H. and Morley, S. C. (2019) ‘Cells under stress: The mechanical environment shapes inflammasome responses to danger signals’, *Journal of Leukocyte Biology*, 106(1), pp. 119–125. doi: 10.1002/JLB.3MIR1118-417R.

Kanie, K. *et al.* (2019) ‘Effect of mechanical vibration stress in cell culture on human induced pluripotent stem cells’, *Regenerative Therapy*. doi: 10.1016/j.reth.2019.05.002.

Kawaguchi, T. (2016) ‘Organ Preference of Cancer Metastasis and Metastasis-Related Cell Adhesion Molecules Including Carbohydrates’, *Cardiovascular & Hematological Disorders-Drug Targets*, 15(3), pp. 164–186. doi: 10.2174/1871529x15666151102102551.

Khalili, A. and Ahmad, M. (2015) ‘A Review of Cell Adhesion Studies for Biomedical and Biological Applications’, *International Journal of Molecular Sciences*, 16(8), pp. 18149–18184. doi: 10.3390/ijms160818149.

Khatau, S. B. *et al.* (2009) ‘A perinuclear actin cap regulates nuclear shape’, *Proceedings of the National Academy of Sciences of the United States of America*, 106(45), pp. 19017–19022. doi: 10.1073/pnas.0908686106.

Kim, D. H., Cho, S. and Wirtz, D. (2014) ‘Tight coupling between nucleus and cell migration through the perinuclear actin cap’, *Journal of Cell Science*, 127(11), pp. 2528–2541. doi: 10.1242/jcs.144345.

Kim, N. G. *et al.* (2011) ‘E-cadherin mediates contact inhibition of proliferation through Hippo signaling-pathway components’, *Proceedings of the National Academy of Sciences of the United States of America*, 108(29), pp. 11930–11935. doi: 10.1073/pnas.1103345108.

Koch, T. M. *et al.* (2012) ‘3D traction forces in cancer cell invasion’, *PLoS ONE*, 7(3). doi: 10.1371/journal.pone.0033476.

Kubben, N. *et al.* (2011) ‘Post-natal myogenic and adipogenic developmental’, *Nucleus*, 2(3), pp. 195–207. doi: 10.4161/nucl.2.3.15731.

Ladoux, B. *et al.* (2010) ‘Strength dependence of cadherin-mediated adhesions’, *Biophysical Journal*, 98(4), pp. 534–542. doi: 10.1016/j.bpj.2009.10.044.

Lammerding, J. *et al.* (2004) ‘Lamin A/C deficiency causes defective nuclear mechanics and mechanotransduction’, *Journal of Clinical Investigation*, 113(3), pp. 370–378. doi: 10.1172/JCI200419670.

Lebaron, R. G. and Athanasiou, K. A. (2000) ‘Ex vivo synthesis of articular cartilage’, *Biomaterials*, 21(24), pp. 2575–2587. doi: 10.1016/S0142-9612(00)00125-3.

Leckband, D. E. *et al.* (2011) ‘Mechanotransduction at cadherin-mediated adhesions’, *Current Opinion in Cell Biology*, 23(5), pp. 523–530. doi: 10.1016/j.ceb.2011.08.003.

Leckband, D. E. and de Rooij, J. (2014) ‘Cadherin Adhesion and Mechanotransduction’, *Annual Review of Cell and Developmental Biology*, 30(1), pp. 291–315. doi: 10.1146/annurev-cellbio-100913-013212.

Lee, W. *et al.* (2014) ‘Synergy between Piezo1 and Piezo2 channels confers high-strain mechanosensitivity to articular cartilage’, *Proceedings of the National Academy*

of Sciences of the United States of America, 111(47), pp. E5114–E5122. doi: 10.1073/pnas.1414298111.

Li, Y. *et al.* (2011) 'Biophysical regulation of histone acetylation in mesenchymal stem cells', *Biophysical Journal*, 100(8), pp. 1902–1909. doi: 10.1016/j.bpj.2011.03.008.

Li, Y. *et al.* (2015) 'Moving Cell Boundaries Drive Nuclear Shaping during Cell Spreading', *Biophysical Journal*, 109(4), pp. 670–686. doi: 10.1016/j.bpj.2015.07.006.

Liu, Z. *et al.* (2010) 'Mechanical tugging force regulates the size of cell-cell junctions', *Proceedings of the National Academy of Sciences of the United States of America*, 107(22), pp. 9944–9949. doi: 10.1073/pnas.0914547107.

Lombardi, M. L. *et al.* (2011) 'The interaction between nesprins and sun proteins at the nuclear envelope is critical for force transmission between the nucleus and cytoskeleton', *Journal of Biological Chemistry*, 286(30), pp. 26743–26753. doi: 10.1074/jbc.M111.233700.

López, J. A. *et al.* (1998) 'Bernard-Soulier syndrome.', *Blood*, 91(12), pp. 4397–418. Available at: http://www.ncbi.nlm.nih.gov/pubmed/9616133.

Lord, M. S. *et al.* (2006) 'Monitoring cell adhesion on tantalum and oxidised polystyrene using a quartz crystal microbalance with dissipation', *Biomaterials*, 27(26), pp. 4529–4537.

Di Loreto, C. *et al.* (2004) 'Effects of whole-body vibration exercise on the endocrine system of healthy men', *Journal of Endocrinological Investigation*, 27(4), pp. 323–327. doi: 10.1007/BF03351056.

Lu, H. *et al.* (2004) 'Microfluidic shear devices for quantitative analysis of cell adhesion', *Analytical Chemistry*, 76(18), pp. 5257–5264. doi: 10.1021/ac049837t.

Lund, E. *et al.* (2013) 'Lamin A/C-promoter interactions specify chromatin state-dependent transcription outcomes', *Genome Research*, 23(10), pp. 1580–1589. doi: 10.1101/gr.159400.113.

M., Z. *et al.* (2013) 'Myopathic lamin mutations impair nuclear stability in cells and tissue and disrupt nucleo-cytoskeletal coupling', *Human Molecular Genetics*, 22(12), pp. 2335–2349. doi: 10.1093/hmg/ddt079 LK - http://limo.libis.be/resolver?&sid=EMBASE&issn=09646906&id=doi:10.1093%2Fhmg%2Fddt079&atitle=Myopathic+lamin+mutations+impair+nuclear+stability+in+cells+and+tissue+and+disrupt+nucleo-cytoskeletal+coupling&stitle=Hum.+Mol.+Genet.&title=Human+Molecular+Genetics&volume=22&issue=12&spage=2335&epage=2349&aulast=Zwerger&aufirst=Monika&auinit=M.&aufull=Zwerger+M.&coden=HMGEE&isbn=&pages=2335-2349&date=2013&auinit1=M&auinitm=.

Machowska, M., Piekarowicz, K. and Rzepecki, R. (2015) 'Regulation of lamin properties and functions: Does phosphorylation do it all?', *Open Biology*, 5(11). doi: 10.1098/rsob.150094.

Maharana, S. *et al.* (2016) 'Chromosome intermingling - The physical basis of chromosome organization in differentiated cells', *Nucleic Acids Research*, 44(11), pp. 5148–5160. doi: 10.1093/nar/gkw131.

Makhija, E., Jokhun, D. S. and Shivashankar, G. V. (2016) 'Nuclear deformability and telomere dynamics are regulated by cell geometric constraints', *Proceedings of the National Academy of Sciences of the United States of America*, 113(1), pp. E32–E40. doi: 10.1073/pnas.1513189113.

Maniotis, A. J., Chen, C. S. and Ingber, D. E. (1997) 'Demonstration of mechanical connections between integrins, cytoskeletal filaments, and nucleoplasm that stabilize nuclear structure', *Proceedings of the National Academy of Sciences of the United States of America*, 94(3), pp. 849–854. doi: 10.1073/pnas.94.3.849.

Marganski, W. A., Dembo, M. and Wang, Y. L. (2003) 'Measurements of cell-generated deformations on flexible substrata using correlation-based optical flow', *Methods in Enzymology*, 361, pp. 197–211. doi: 10.1016/S0076-6879(03)61012-8.

Marx, K. A. *et al.* (2007) 'A comparative study of the cytoskeleton binding drugs nocodazole and taxol with a mammalian cell quartz crystal microbalance biosensor: Different dynamic responses and energy dissipation effects', *Analytical Biochemistry*, 361(1), pp. 77–92. doi: 10.1016/j.ab.2006.09.023.

Mianabadi, M. and Yazdanparast, R. (2004) 'Inhibition of substrate-tumor cell adhesion under the effect of gnidilatimonoein purified from Daphne mucronata', *American Journal of Chinese Medicine*, 32(3), pp. 369–376. doi: 10.1142/S0192415X04002028.

Michael, K. E. *et al.* (2009) 'Focal adhesion kinase modulates cell adhesion strengthening via integrin activation', *Molecular Biology of the Cell*, 20(9), pp. 2508–2519. doi: 10.1091/mbc.E08-01-0076.

Misteli, T. (2007) 'Beyond the Sequence: Cellular Organization of Genome Function', *Cell*, 128(4), pp. 787–800. doi: 10.1016/j.cell.2007.01.028.

Mueller, M. J. and Maluf, K. S. (2002) 'Tissue Adaptation to Physical Stress: A Proposed "Physical Stress Theory" to Guide Physical Therapist Practice, Education, and Research', *Physical Therapy*, 82(4), pp. 383–403. doi: 10.1093/ptj/82.4.383.

Multicomp (2014) 'MCABT-455-RC Piezo Element Datasheet', (V1.1). Available at: http://uk.farnell.com/multicomp/mcft-27t-4-2al-127/piezo-element/dp/1801061.

Murphy, A. J. *et al.* (2014) 'Aberrant activation, nuclear localization, and phosphorylation of yes-associated protein-1 in the embryonic kidney and Wilms tumor', *Pediatric Blood & Cancer*, 61(2), pp. 198–205. doi: 10.1002/pbc.24788.

Neelam, S. *et al.* (2015) 'Direct force probe reveals the mechanics of nuclear homeostasis in the mammalian cell', *Proceedings of the National Academy of Sciences of the United States of America*, 112(18), pp. 5720–5725. doi: 10.1073/pnas.1502111112.

Nelson, C., Rabb, H. and Arnaout, M. A. (1992) 'Genetic cause of leukocyte adhesion molecule deficiency. Abnormal splicing and a missense mutation in a conserved region of CD18 impair cell surface expression of beta 2 integrins.', *The Journal of biological chemistry*, 267(5), pp. 3351–7. Available at: http://www.ncbi.nlm.nih.gov/pubmed/1346613.

Niessen, C. M., Leckband, D. and Yap, A. S. (2011) 'Tissue organization by cadherin adhesion molecules: Dynamic Molecular and Cellular Mechanisms of Morphogenetic Regulation', *Physiological Reviews*, 91(2), pp. 691–731. doi: 10.1152/physrev.00004.2010.

O'Conor, C. J. *et al.* (2014) 'TRPV4-mediated mechanotransduction regulates the metabolic response of chondrocytes to dynamic loading', *Proceedings of the National Academy of Sciences of the United States of America*, 111(4), pp. 1316–1321. doi: 10.1073/pnas.1319569111.

Pajerowski, J. D. *et al.* (2007) 'Physical plasticity of the nucleus in stem cell differentiation', *Proceedings of the National Academy of Sciences of the United States of America*, 104(40), pp. 15619–15624. doi: 10.1073/pnas.0702576104.

Park, J. Y., Amin Arnaout, M. and Gupta, V. (2007) 'A simple, no-wash cell adhesion-based high-throughput assay for the discovery of small-molecule regulators of the integrin CD11b/CD18', *Journal of Biomolecular Screening*, 12(3), pp. 406–417. doi: 10.1177/1087057106299162.

Pathak, M. M. *et al.* (2014) 'Stretch-activated ion channel Piezo1 directs lineage choice in human neural stem cells', *Proceedings of the National Academy of Sciences of the United States of America*, 111(45), pp. 16148–16153. doi: 10.1073/pnas.1409802111.

Pauli, B. U. *et al.* (1990) 'Organ-preference of metastasis', *CANCER AND METASTASIS REVIEW*, 9(3), pp. 175–189. doi: 10.1007/BF00046359.

Peric-Hupkes, D. *et al.* (2010) 'Molecular Maps of the Reorganization of Genome-Nuclear Lamina Interactions during Differentiation', *Molecular Cell*, 38(4), pp. 603–613. doi: 10.1016/j.molcel.2010.03.016.

Petrova, Y. I., Spano, M. M. and Gumbiner, B. M. (2012) 'Conformational epitopes at cadherin calcium-binding sites and p120-catenin phosphorylation regulate cell adhesion', *Molecular Biology of the Cell*. Edited by A. Nusrat, 23(11), pp. 2092–2108. doi: 10.1091/mbc.e11-12-1060.

PI Ceramic GmbH (2014) 'Piezoelectric Ceramic Products', pp. 1–44.

Poh, Y. C. *et al.* (2012) 'Dynamic force-induced direct dissociation of protein complexes in a nuclear body in living cells', *Nature Communications*, 3. doi: 10.1038/ncomms1873.

Pokutta, S. *et al.* (1994) 'Conformational changes of the recombinant extracellular domain of E-cadherin upon calcium binding', *European Journal of Biochemistry*, 223(3), pp. 1019–1026. doi: 10.1111/j.1432-1033.1994.tb19080.x.

Pollard, T. D. (2017) *Cell Biology, 3rd edition*. Elsevier.

Priest, A. V., Shafraz, O. and Sivasankar, S. (2017) 'Biophysical basis of cadherin mediated cell-cell adhesion', *Experimental Cell Research*. Elsevier Inc., 358(1), pp. 10–13. doi: 10.1016/j.yexcr.2017.03.015.

Ragoczy, T. *et al.* (2006) 'The locus control region is required for association of the murine β-globin locus with engaged transcription factories during erythroid maturation', *Genes and Development*, 20(11), pp. 1447–1457. doi: 10.1101/gad.1419506.

Raibon, E. and Möller, T. (2009) 'Microglia Identification Methods', *Encyclopedia of Neuroscience*, pp. 849–852. doi: 10.1016/B978-008045046-9.01752-6.

Reddy, K. L. *et al.* (2008) 'Transcriptional repression mediated by repositioning of genes to the nuclear lamina', *Nature*, 452(7184), pp. 243–247. doi: 10.1038/nature06727.

Reyes, C. D. and García, A. J. (2003) 'A centrifugation cell adhesion assay for high-throughput screening of biomaterial surfaces', *Journal of Biomedical Materials Research - Part A*, 67(1), pp. 328–333. doi: 10.1002/jbm.a.10122.

Rolke, R. *et al.* (2013) 'Hand-arm vibration syndrome: Clinical characteristics, conventional electrophysiology and quantitative sensory testing', *Clinical Neurophysiology*, 124(8), pp. 1680–1688. doi: 10.1016/j.clinph.2013.01.025.

Le Roux, A. L. *et al.* (2019) 'The plasma membrane as a mechanochemical transducer', *Philosophical Transactions of the Royal Society B: Biological Sciences*, 374(1779). doi: 10.1098/rstb.2018.0221.

Rupprecht, P. *et al.* (2012) 'A tapered channel microfluidic device for comprehensive

cell adhesion analysis, using measurements of detachment kinetics and shear stress-dependent motion', *Biomicrofluidics*, 6(1). doi: 10.1063/1.3673802.

Rustad, K. C., Wong, V. W. and Gurtner, G. C. (2013) 'The role of focal adhesion complexes in fibroblast mechanotransduction during scar formation.', *Differentiation; research in biological diversity*. England, 86(3), pp. 87–91. doi: 10.1016/j.diff.2013.02.003.

Sáez, J. C. *et al.* (2003) 'Plasma membrane channels formed by connexins: Their regulation and functions', *Physiological Reviews*, 83(4), pp. 1359–1400. doi: 10.1152/physrev.00007.2003.

Saitou, M. *et al.* (2000) 'Complex Phenotype of Mice Lacking Occludin, a Component of Tight Junction Strands', *Molecular Biology of the Cell*. Edited by W. J. Nelson, 11(12), pp. 4131–4142. doi: 10.1091/mbc.11.12.4131.

Sawada, Y. *et al.* (2006) 'Force Sensing by Mechanical Extension of the Src Family Kinase Substrate p130Cas', *Cell*, 127(5), pp. 1015–1026. doi: 10.1016/j.cell.2006.09.044.

Schlegelmilch, K. *et al.* (2011) 'Yap1 acts downstream of α-catenin to control epidermal proliferation', *Cell*, 144(5), pp. 782–795. doi: 10.1016/j.cell.2011.02.031.

Sexton, T. *et al.* (2007) 'Gene regulation through nuclear organization', *Nature Structural and Molecular Biology*, 14(11), pp. 1049–1055. doi: 10.1038/nsmb1324.

Sluchanko, N. N. and Gusev, N. B. (2010) '14-3-3 Proteins and regulation of cytoskeleton', *Biochemistry (Moscow)*, 75(13), pp. 1528–1546. doi: 10.1134/S0006297910130031.

Solon, J. *et al.* (2007) 'Fibroblast adaptation and stiffness matching to soft elastic substrates', *Biophysical Journal*, 93(12), pp. 4453–4461. doi: 10.1529/biophysj.106.101386.

Song, J. W. *et al.* (2009) 'Microfluidic endothelium for studying the intravascular adhesion of metastatic breast cancer cells', *PLoS ONE*, 4(6). doi: 10.1371/journal.pone.0005756.

Sun, Y. *et al.* (2014) 'Hippo/YAP-mediated rigidity-dependent motor neuron differentiation of human pluripotent stem cells', *Nature Materials*, 13(6), pp. 599–604. doi: 10.1038/nmat3945.

Sweeney, H. L. *et al.* (2006) 'Matrix elasticity directs stem cell lineage specification', *Cell*.

Swift, J. *et al.* (2013) 'Nuclear lamin-A scales with tissue stiffness and enhances matrix-directed differentiation', *Science*, 341(6149). doi: 10.1126/science.1240104.

Swift, J. and Discher, D. E. (2014) 'The nuclear lamina is mechano-responsive to ECM elasticity in mature tissue', *Journal of Cell Science*, 127(14), pp. 3005–3015. doi: 10.1242/jcs.149203.

Szczerbal, I., Foster, H. A. and Bridger, J. M. (2009) 'The spatial repositioning of adipogenesis genes is correlated with their expression status in a porcine mesenchymal stem cell adipogenesis model system', *Chromosoma*, 118(5), pp. 647–663. doi: 10.1007/s00412-009-0225-5.

Szczesny, S. E. and Mauck, R. L. (2016) 'The Nuclear Option: Evidence Implicating the Cell Nucleus in Mechanotransduction', *Journal of Biomechanical Engineering*, 139(2), p. 021006. doi: 10.1115/1.4035350.

T, C. and C, C. (2001) ‘Chromosome territories, nuclear architecture and gene regulation in mammalian cells’, *Nature Reviews Genetics*, 2(April), pp. 292–301.

Tajik, A. *et al.* (2016) ‘Transcription upregulation via force-induced direct stretching of chromatin’, *Nature Materials*, 15(12), pp. 1287–1296. doi: 10.1038/nmat4729.

Tang, Z. *et al.* (2012) ‘Shear stress-dependent cell detachment from temperature-responsive cell culture surfaces in a microfluidic device’, *Biomaterials*, 33(30), pp. 7405–7411. doi: 10.1016/j.biomaterials.2012.06.077.

Thomas, W. A. *et al.* (2013) ‘α-Catenin and vinculin cooperate to promote high E-cadherin-based adhesion strength’, *Journal of Biological Chemistry*, 288(7), pp. 4957–4969. doi: 10.1074/jbc.M112.403774.

Tirkkonen, L. *et al.* (2011) ‘The effects of vibration loading on adipose stem cell number, viability and differentiation towards bone-forming cells’, *Journal of the Royal Society Interface*, 8(65), pp. 1736–1747. doi: 10.1098/rsif.2011.0211.

Titze, I. R. (1989) ‘On the relation between subglottal pressure and fundamental frequency in phonation’, *The Journal of the Acoustical Society of America*, 85(2), pp. 901–906. doi: 10.1121/1.397562.

Topolov, V. Y., Bowen, C. R. and Bisegna, P. (2018a) *Piezo-Active Composites*. Cham: Springer International Publishing (Springer Series in Materials Science). doi: 10.1007/978-3-319-93928-5.

Topolov, V. Y., Bowen, C. R. and Bisegna, P. (2018b) ‘The Piezoelectric Medium and Piezoelectric Sensitivity’, in, pp. 1–34. doi: 10.1007/978-3-319-93928-5_1.

Townes, P. L. and Holtfreter, J. (1955) ‘Directed movements and selective adhesion of embryonic amphibian cells’, *Journal of Experimental Zoology*, 128(1), pp. 53–120. doi: 10.1002/jez.1401280105.

Tse, J. R. and Engler, A. J. (2011) ‘Stiffness gradients mimicking in vivo tissue variation regulate mesenchymal stem cell fate’, *PLoS ONE*, 6(1). doi: 10.1371/journal.pone.0015978.

Tsimbouri, P. M. *et al.* (2017) ‘Stimulation of 3D osteogenesis by mesenchymal stem cells using a nanovibrational bioreactor’, *Nature Biomedical Engineering*, 1(9), pp. 758–770. doi: 10.1038/s41551-017-0127-4.

U.S. Department of Health and Human Services (no date) *2008 Physical Activity Guidelines for Americans*, *2008*. Available at: https://health.gov/paguidelines/2008/ (Accessed: 19 August 2019).

Ullrich, N. *et al.* (2019) ‘The role of mechanotransduction versus hypoxia during simulated orthodontic compressive strain—an in vitro study of human periodontal ligament fibroblasts’, *International Journal of Oral Science*, 11(4), p. 33. doi: 10.1038/s41368-019-0066-x.

Usami, S. *et al.* (1993) ‘Design and construction of a linear shear stress flow chamber’, *Annals of Biomedical Engineering*, 21(1), pp. 77–83. doi: 10.1007/BF02368167.

Vendome, J. *et al.* (2011) ‘Molecular design principles underlying βstrand swapping in the adhesive dimerization of cadherins’, *Nature Structural and Molecular Biology*, 18(6), pp. 693–700. doi: 10.1038/nsmb.2051.

Vincent, L. G. *et al.* (2013) ‘Mesenchymal stem cell durotaxis depends on substrate stiffness gradient strength’, *Biotechnology Journal*, 8(4), pp. 472–484. doi: 10.1002/biot.201200205.

Vining, K. H. and Mooney, D. J. (2017) ‘Mechanical forces direct stem cell behaviour in development and regeneration’, *Nature Reviews Molecular Cell Biology*. Nature Publishing Group, pp. 728–742. doi: 10.1038/nrm.2017.108.

Vogel, J. *et al.* (1998) ‘The role of glycolipids in mediating cell adhesion: A flow chamber study’, *Biochimica et Biophysica Acta - Biomembranes*, 1372(2), pp. 205–215. doi: 10.1016/S0005-2736(98)00058-3.

Wagner, A. P. *et al.* (2016) ‘Vibratory stimulation enhances thyroid epithelial cell function’, *Biochemistry and Biophysics Reports*. Elsevier, 8(April), pp. 376–381. doi: 10.1016/j.bbrep.2016.10.008.

Wallrath, L. L., Bohnekamp, J. and Magin, T. M. (2016) ‘Cross talk between the cytoplasm and nucleus during development and disease’, *Current Opinion in Genetics and Development*. Elsevier Ltd, 37, pp. 129–136. doi: 10.1016/j.gde.2016.03.007.

Wang, N., Tytell, J. D. and Ingber, D. E. (2009) *Mechanotransduction at a distance: Mechanically coupling the extracellular matrix with the nucleus*, *Nature Reviews Molecular Cell Biology*. doi: 10.1038/nrm2594.

Whitney O, L. *et al.* (2012) ‘Parallel-plate flow chamber and continuous flow circuit to evaluate endothelial progenitor cells under laminar flow shear stress’, *Journal of Visualized Experiments*, (59). Available at: http://www.jove.com/video/3349/parallel-plate-flow-chamber-and-continuous-flow-circuit-to-evaluate-endothelial-progenitor-cells-under-laminar-flow-shear-stress%5Cnfiles/201/parallel-plate-flow-chamber-continuous-flow-circuit-to-evaluate.html.

Wilson, K. L. and Foisner, R. (2010) ‘Lamin-binding Proteins.’, *Cold Spring Harbor perspectives in biology*, 2(4). doi: 10.1101/cshperspect.a000554.

Yan, J. *et al.* (2015) ‘Talin Dependent Mechanosensitivity of Cell Focal Adhesions’, *Cellular and Molecular Bioengineering*, 8(1), pp. 151–159. doi: 10.1007/s12195-014-0364-5.

Yao, J. *et al.* (2011) ‘Subnuclear segregation of genes and core promoter factors in myogenesis’, *Genes and Development*, 25(6), pp. 569–580. doi: 10.1101/gad.2021411.

Yonemura, S. *et al.* (2010) ‘α-Catenin as a tension transducer that induces adherens junction development’, *Nature Cell Biology*, 12(6), pp. 533–542. doi: 10.1038/ncb2055.

Yonemura, S. (2011) ‘A mechanism of mechanotransduction at the cell-cell interface’, *BioEssays*, 33(10), pp. 732–736. doi: 10.1002/bies.201100064.

Zhang, C. *et al.* (2012) ‘Effects of mechanical vibration on proliferation and osteogenic differentiation of human periodontal ligament stem cells’, *Archives of Oral Biology*, 57(10), pp. 1395–1407. doi: 10.1016/j.archoralbio.2012.04.010.

Zhou, A. X., Hartwig, J. H. and Akyürek, L. M. (2010) ‘Filamins in cell signaling, transcription and organ development’, *Trends in Cell Biology*, 20(2), pp. 113–123. doi: 10.1016/j.tcb.2009.12.001.

APPENDIX A: CODE TO RUN ADXL345 ACCELEROMETER

```
#include "timed_measurement.h"   // Only defines setupFIFO and idle
functions elsewhere for coding clarity here
#include "SparkFun_ADXL345.h"    // SparkFun’s ADXL345 library
#include "Wire.h"                // Arduino device communication
#define ADDR 0x53                // Device address



// MODIFY THESE VALUES FOR DIFFERENT EFFECTS

unsigned long shockInterval = 100;        // limits piezo shocks to
happen once every designated amount of milliseconds at most, will not
happen exactly at this interval depending processing speed, timerOn
must be true to take effect
int sampleDelay = 5;                      // milliseconds between
samples, lower value means greater accuracy
int samplesPerStimulation = 1;            // values in fifo will be
recorded this many times between piezo "shocks", if timer in use
program will wait for the designated period AND collect this amount of
samples before generating another shock
int sampleAccuracy = 8;                   // Only put values 2,4,8 or
16 , controls sample accuracy, 2 means most accurate however only
acceleration up to 2g etc.
int sampleAmount = 1000;                   // how many samples will
be taken per measurement
int fifoReadAmount = 32;                  // how many values will be
read per fifo record max is 32
bool timerOn = true;                      // true if timer desired,
false otherwise

// DON'T TOUCH THESE
int  x, y, z;                                              // raw
acceleration values
int piezoForce;                                            // stores
acceleration value
int sampleCount;                                           // tracks
timing in the program
int averageAmbientY, averageAmbientX, averageAmbientZ;     // stores
calibration values
int forceBig;                                              // stores
the highest value
int sampleTaken;                                           // stores
amount of samplestaken
int toggle;                                                // piezo
toggle
float forceMultiplier2g = 3.9;                             // modified
as specified in the adxl345 datasheet
float forceMultiplier4g = 7.8;
float forceMultiplier8g = 15.6;
float forceMultiplier16g = 31.2;
float forceMultiplier;                // scaling variable
unsigned long timeElapsedLastShock;   // timing variable
long int xSize, ySize, zSize;         // holder variable

bool calibDone = false;    // tracks calibration
```

```
bool valuesSet = false;    // tracks values
ADXL345 adxl = ADXL345();  // defined accelerometer


// SETUP
void setup() {
  // put your setup code here, to run once:
  Serial.begin(115200);           // starts communication between
computer and the device on this frequency, data will be stored on the
serial monitor on this frequency

  adxl.powerOn();
  adxl.setRangeSetting(sampleAccuracy);
  adxl.set_bw(ADXL345_BW_1600);    // set bandwidth to 1600 Hz
  pinMode(A3, OUTPUT);             // Setting the output pins for the
piezos

  setupFIFO();

  if(sampleAccuracy == 2){  // sets the values to be correct for the
chosen measurement accuracy
    forceMultiplier = forceMultiplier2g;
  } else if (sampleAccuracy == 4){
    forceMultiplier = forceMultiplier4g;
  } else if (sampleAccuracy == 8){
    forceMultiplier = forceMultiplier8g;
  } else if (sampleAccuracy == 16){
    forceMultiplier = forceMultiplier16g;
  } else{
    Serial.println("Please put only values 2,4,8 or 16 as sample
accuracy");
    idle();                         // device will idle
    }


}

// MAIN PROCESS
void loop() {
  // put your main code here, to run repeatedly:

  if (calibDone == false) {

    delay(1000);
    for (int k = 0; k < 32; k++) {
      adxl.readAccel(&x, &y, &z);                         // eliminates
outside forces from results
      averageAmbientZ += z * forceMultiplier;
      averageAmbientX += x * forceMultiplier;
      averageAmbientY += y * forceMultiplier;
    }
    averageAmbientZ = averageAmbientZ * 1 / 32;
    averageAmbientX = averageAmbientX * 1 / 32;
    averageAmbientY = averageAmbientY * 1 / 32;
    calibDone = true;
  }


  if (sampleCount > samplesPerStimulation ) {
```

```
    if ( millis() - timeElapsedLastShock > shockInterval or timerOn ==
false) {   //checks if timer is on and if the specified time between
shocks has passed
      if (toggle > 0) {
        toggle = 0;                          // generates piezo shock
        digitalWrite(A3, HIGH);
      }
      else {
        toggle = 1;
        digitalWrite(A3, LOW);
      }
       timeElapsedLastShock = millis();


    }
    sampleCount = 0;

  }

  for (int i = 0; i < fifoReadAmount; i++) {
    delay(sampleDelay);   //
    adxl.readAccel(&x, &y, &z);

    zSize = z * forceMultiplier - averageAmbientZ;
    xSize = x * forceMultiplier - averageAmbientX;
    ySize = y * forceMultiplier - averageAmbientY;

    piezoForce = abs(sqrt(pow(sqrt(ySize * ySize + xSize * xSize), 2)
+ zSize * zSize));                  // resultant force calculated
using Pythagorean theorem



    if (valuesSet == false or forceBig < piezoForce) {
      forceBig = piezoForce;                                    //
stores the highest force in a measurement
    }

    Serial.print(piezoForce);
    Serial.print(" ");
    Serial.println(forceBig);
    valuesSet = true;

  }



  sampleTaken++;
  if (sampleTaken >= sampleAmount){

    idle();
  }
  sampleCount++;
}



// timed_measurement.h to be run as a separate file

//#ifndef timedMeasurement
```

```
//#define timedMeasurement

//void setupFIFO();
//void idle();

//#endif
```

APPENDIX B: YAP ANALYSIS RESULTS

17.2.2020
Arno Pammo / Vibration experiments / Elina M stainings
MDCK II wt p10
Centre plain, 5 fields
AM488/YAP63.7
Phalloidin 565
AR647 / Cx43 rabbit

CH1: DAPI, median filtering radius 2, adjust threshold, convert to mask
CH2: Gaussian filtering radius 1, measure from created mask

ANALYSIS OF NUCLEOPLASMIC YAP63.7 — **Nucleus**

Area	Name	Order	Area	Mean	StdDev	Circ.	AR	Round	Solidity
MIDDLE	Control	1	20035,329	96,266	24,13	0,005	1,036	0,965	0,446
		1	21461,363	99,942	25,634	0,005	1,025	0,976	0,478
		1	23352,942	86,847	30,355	0,004	1,018	0,982	0,52
		1	21624,227	96,918	25,331	0,005	1,027	0,974	0,481
		1	22178,95	82,028	22,903	0,005	1,03	0,971	0,498
	Mean		**21730,5622**	**92,4002**	**25,6706**	**0,0048**	**1,0272**	**0,9736**	**0,4846**
MIDDLE	MDCK- 1h Recovery from Vibration 1	1	19384,217	102,295	24,491	0,006	1,046	0,956	0,432
		1	20327,711	86,336	22,045	0,005	1,055	0,947	0,452
		1	17102,065	95,605	28,537	0,005	1,047	0,955	0,38
		1	20011,168	98,479	26,844	0,005	1,022	0,978	0,446
		1	19788,051	90,892	25,463	0,005	1,019	0,982	0,44
	Mean		**19322,6424**	**94,7214**	**25,476**	**0,0052**	**1,0378**	**0,9636**	**0,43**
EDGE	MDCK- 1h Recovery from Vibration 2	1	19057,932	100,318	25,363	0,005	1,094	0,914	0,427
		1	19262,295	101,616	25,26	0,005	1,026	0,974	0,428
		1	17940,888	111,018	28,995	0,006	1,066	0,938	0,4
		1	19570,169	100,833	26,735	0,005	1,024	0,977	0,435
		1	18786,707	101,623	25,415	0,005	1,06	0,943	0,422
	Mean		**18923,5982**	**103,0816**	**26,3536**	**0,0052**	**1,054**	**0,9492**	**0,4224**
MIDDLE	MDCK- 2hRecovery from Vibration 1	1	22616,515	83,868	21,98	0,004	1,031	0,97	0,505
		1	20924,363	65,472	20,579	0,004	1,06	0,943	0,465
		1	20707,04	89,35	22,384	0,005	1,046	0,956	0,461
		1	18915,453	96,805	23,721	0,006	1,068	0,937	0,422
		1	19738,698	91,646	22,065	0,005	1,047	0,955	0,442
	Mean		**20580,4138**	**85,4282**	**22,1458**	**0,0048**	**1,0504**	**0,9522**	**0,459**
EDGE	MDCK- 2hRecovery from Vibration 1	1	18346,395	81,351	22,732	0,006	1,025	0,976	0,408
		1	20051,894	91,033	24,39	0,005	1,093	0,915	0,446
		1	20184,717	85,732	26,034	0,005	1,079	0,927	0,453
		1	19036,474	82,679	22,662	0,005	1,086	0,921	0,426

		1	18044,529	88,512	24,773	0,005	1,079	0,927	0,403
	Mean		**19132,8018**	**85,8614**	**24,1182**	**0,0052**	**1,0724**	**0,9332**	**0,4272**

			Cytoplasm						
Area	**Name**	**Order**	**Area**	**Mean**	**StdDev**	**Circ.**	**AR**	**Round**	**Solidity**
MIDDLE	Control	2	24964,671	102,958	34,569	0,006	1,026	0,975	0,555
		2	23538,637	87,95	37,181	0,005	1,021	0,979	0,524
		2	21647,058	98,244	30,266	0,004	1,024	0,976	0,481
		2	23375,773	107,367	26,694	0,005	1,023	0,978	0,52
		2	22821,05	84,49	27,989	0,005	1,028	0,973	0,508
	Mean		**23269,4378**	**96,2018**	**31,3398**	**0,005**	**1,0244**	**0,9762**	**0,5176**
MIDDLE	MDCK 1h Recovery from Vibration 1	2	25615,783	92,594	32,235	0,007	1,031	0,97	0,569
		2	24672,289	75,802	30,792	0,006	1,041	0,96	0,548
		2	27897,935	97,584	32,713	0,008	1,028	0,973	0,62
		2	24988,832	106,988	30,251	0,006	1,018	0,982	0,556
		2	25211,949	90,272	30,228	0,006	1,013	0,988	0,56
	Mean		**25677,3576**	**92,648**	**31,2438**	**0,0066**	**1,0262**	**0,9746**	**0,5706**
EDGE	MDCK 1h Recovery from Vibration 2	2	25942,068	96,007	32,474	0,007	1,059	0,944	0,577
		2	25737,705	88,768	38,28	0,006	1,014	0,987	0,572
		2	27059,112	96,112	34,229	0,009	1,042	0,96	0,602
		2	25429,831	102,29	35,028	0,006	1,018	0,982	0,566
		2	26213,293	99,701	35,03	0,007	1,037	0,964	0,583
	Mean		**26076,4018**	**96,5756**	**35,0082**	**0,007**	**1,034**	**0,9674**	**0,58**
MIDDLE	MDCK 2h Recovery from Vibration 1	2	22383,485	93,737	26,701	0,004	1,031	0,97	0,498
		2	24075,637	65,598	23,338	0,005	1,062	0,941	0,536
		2	24292,96	92,91	30,467	0,005	1,032	0,969	0,54
		2	26084,547	91,016	29,801	0,007	1,048	0,954	0,58
		2	25261,302	100,874	29,101	0,006	1,035	0,966	0,562
	Mean		**24419,5862**	**88,827**	**27,8816**	**0,0054**	**1,0416**	**0,96**	**0,5432**
EDGE	MDCK 2h Recovery from Vibration 1	2	26653,605	79,56	26,794	0,008	1,02	0,981	0,593
		2	24948,106	92,282	35,59	0,006	1,067	0,937	0,556
		2	24815,283	99,029	29,477	0,006	1,057	0,946	0,552
		2	25963,526	89,809	28,076	0,007	1,06	0,943	0,577
		2	26955,471	86,346	33,183	0,007	1,046	0,956	0,599
	Mean		**25867,1982**	**89,4052**	**30,624**	**0,0068**	**1,05**	**0,9526**	**0,5754**

		YAP Intensity	
		NP/CP	MEAN
Area	Name		

MIDDLE	Control	0,935002622	
		1,136350199	
		0,883992916	**0,965777158**
		0,902679594	
		0,970860457	
MIDDLE	MDCK 1hRecovery from Vibration 1	1,104769208	
		1,13896731	
		0,979720036	**1,03015848**
		0,920467716	
		1,006868132	
EDGE	MDCK 1h Recovery from Vibration 2	1,044902976	
		1,144736842	
		1,155089895	**1,069952707**
		0,985756183	
		1,01927764	
MIDDLE	MDCK 2h Recovery from Vibration 1	0,894716067	
		0,99807921	
		0,961683349	**0,965320473**
		1,063604201	
		0,908519539	
EDGE	MDCK 2h Recovery from Vibration 1	1,022511312	
		0,9864654	
		0,865726201	**0,964079466**
		0,920609293	
		1,025085123	

T-tests

Mean nuclear YAP intensity:

	CTRL
CTRL	
1h Recov Middle	0,612940614
1h Recov Edge	0,032539405
2h Recov Middle	0,312236165
2h Recov Edge	0,138940518

Mean cytoplasmic YAP intensity:

	CTRL
CTRL	
1h Recov Middle	0,610832201
1h Recov Edge	0,941865612
2h Recov Middle	0,353991915
2h Recov Edge	0,248019002

STDEV nucleus

	CTRL
CTRL	

STDEV cytoplasm

	CTRL
CTRL	

1h Recov Middle	0,910404211	1h Recov Middle	0,964599757
1h Recov Edge	0,654317021	1h Recov Edge	0,147932367
2h Recov Middle	0,047016945	2h Recov Middle	0,188542797
2h Recov Edge	0,316645579	2h Recov Edge	0,787997529

NP/CP ratio

	CTRL
CTRL	
1h Recov Middle	0,318876682
1h Recov Edge	0,105308383
2h Recov Middle	0,993561769
2h Recov Edge	0,976115926

OUTCOME:

No differences in YAP distribution

No differences in Nucleus shape